



1 **Reviews and syntheses: Methane biogeochemistry in Sundarbans mangrove ecosystem, NE coast**
2 **of India; a box modeling approach**

3 **Manab Kumar Dutta^{1*}, Sandip Kumar Mukhopadhyay²**

4 ¹Geoscience Division, Physical Research Laboratory, Ahmedabad – 380009, India

5 ²Department of Marine Science, University of Calcutta. 35, Ballygunge Circular Road, Kolkata -
6 700019, West Bengal, India

7 ***Author for correspondence:** Postdoctoral Fellow. Geoscience Division, Physical Research
8 Laboratory, Ahmedabad – 380009, India. Email: manabdutta.1987@gmail.com

9 **Abstract:**

10 Biogeochemical cycling of CH₄ was studied in Sundarbans mangrove system during June 2010 to
11 December 2012. The sediment was CH₄ supersaturated with mean production potential of 3547 &
12 48.88 μmol m⁻³ d⁻¹, respectively in case of intertidal (0 – 25 cm depth) & sub-tidal sediments (first 5
13 cm depth). This induces significant CH₄ out-flux from sediment to estuary via advective and diffusive
14 transports. Mean advective (from intertidal sediment) and diffusive (from sub-tidal sediment) CH₄
15 fluxes were 159.52 μmol m⁻² d⁻¹ and 8.45 μmol m⁻² d⁻¹, respectively. Intertidal sediment CH₄ emission
16 rate was about 4 times higher than surface layer CH₄ oxidation rate; indicating petite methanotrophic
17 activity in mangrove sediment. Mean CH₄ concentration in estuarine surface and bottom waters were



18 69.90 and 56.17nM, respectively. CH₄ oxidation in estuarine water column being 14 times higher than
19 water - atmosphere exchange is considered as principal CH₄ removal mechanism in this estuary. Mean
20 CH₄ mixing ratio over the mangrove forest atmosphere was 2.013ppmv. The ecosystem acts a source
21 of CH₄ to the upper atmosphere having mean biosphere - atmosphere exchange flux of 0.086 mg m⁻²
22 d⁻¹. Mean CH₄ photo-oxidation rate in the mangrove forest atmosphere was 3.25 x 10⁻⁹ mg cm⁻³ d⁻¹
23 and is considered as principal CH₄ removal mechanism in the forest atmosphere. Finally, a box model
24 presenting CH₄ biogeochemistry in Sundarbans biosphere reserve has been drafted and was used to
25 demonstrate CH₄ budget in this ecosystem.

26 Keywords: methane, biogeochemistry, budget, mangrove, Sundarbans, India.

27 **1. Introduction:**

28 Methane (CH₄) is the key gaseous constituent of global carbon biogeochemical cycle in anaerobic
29 environment. In carbon biogeochemical cycle, quantitatively 1% of the CO₂ fixed annually by
30 photosynthesis is converted back to CO₂ by microorganisms via CH₄; the amount of CH₄ annually
31 cycled in this way is around 1 billion tones (Rudolf et al. 2006). The atmospheric CH₄ mixing ratio
32 increased from 0.72 ppbv in 1750 to 1.77 ppbv in 2005 (IPCC, 2007); creating a potential threat
33 towards earth's climate as CH₄ global warming potential is 26 times higher than CO₂ (Lelieveld et al.
34 1993). The cause of this large augmentation is not fully understood, but it is probably related to a surge



35 in CH₄ emission from wetlands that contributes approximately 20 - 39% of the annual global CH₄
36 budget (Hoehler et al. 2014).

37 Presenting accurate wetland CH₄ budget is very important for projecting the future climate. But, the
38 primary problems in attempting to develop accurate CH₄ budget is the large spatial and temporal (Ding
39 et al. 2003) variability in CH₄ emissions that reported all over the world. Being an integrated part of
40 coastal wetlands, mangroves are relatively very less studied ecosystem with respect to CH₄
41 biogeochemistry (Barnes et al. 2006; Biswas et al. 2007; Bouillon et al. 2007c; Kristensen et al. 2008).
42 Consequently, presenting wider CH₄ and carbon budgets for mangrove ecosystem globally is
43 problematic.

44 Mangroves are one of the most productive coastal ecosystems and are characterized by high turnover
45 rates of organic matter, both in the water column and in sediment. The organic matter mineralization in
46 sediment is a multi-step process, which begins with an enzymatic hydrolysis of polymeric material to
47 soluble monomeric and oligomeric compounds. Under oxic conditions the organic carbon (OC) is
48 directly mineralized to carbon dioxide and water. But, the mangrove sediments are rich in clay content
49 that reduces the porosity of the sediment and helps in the formation and retention of anoxic condition
50 (Dutta et al. 2013). OC mineralization in anaerobic environment is typically complex involving various
51 microbes in initial de-polymerization followed by fermentative microbial break down of complex
52 organic compounds to small moieties. The end products of the fermentation process used by
53 methanogens in the final step of anaerobic decomposition can also be used by microbial groups that



54 utilize a variety of inorganic terminal electron acceptors (TEAs) in their metabolism (Megonigal et al.
55 2004). The competitiveness, and thus relative importance, of these TEAs is thought to be controlled
56 primarily by their thermodynamic favourability in the following order: NO_3^- (denitrification), Fe (III)
57 (iron reduction), Mn (III, IV) (manganese reduction), and SO_4^{2-} (sulphate reduction) (Keller et al., 2013).
58 Methanogenesis remains suppressed by more favourable TEA-reducing processes and begins when all
59 those TEAs have been consumed and electron donors are in surplus. In fact CH_4 is produced by
60 fermentative disproportionation reaction of low molecular compounds (e.g. acetate) or reduction of CO_2
61 by hydrogen or simple alcohols (Canfield et al. 2005) depending upon redox condition of sediment,
62 which is reported to be ≤ 150 mV for the process of methanogenesis (Wang et al. 1993). The
63 sedimentary produced CH_4 partially escapes through diffusion and direct ebullition to the atmosphere
64 after partially being oxidized at surface (aerobic oxidation) and subsurface sediments (anaerobic
65 oxidation), while the remaining dissolves in pore water resulting super-saturation. During low tide
66 condition, the CH_4 rich pore water transports to the adjacent creeks and estuaries depending upon
67 hypsometric gradient. In addition, CH_4 produced in the underlying sediment of the estuary (sub-tidal
68 sediment) diffuses upward to further enrich the dissolved CH_4 level in estuarine water column.

69 In the estuarine water column, the supplied CH_4 is partly oxidized to CO_2 by methanotrophs, which use
70 CH_4 as the sole carbon source (Hanson and Hanson, 1996). Aerobic CH_4 oxidation in the aquatic
71 systems significantly reduces the CH_4 flux across water – atmosphere interface. In case of stratified
72 systems like lakes, pelagic CH_4 oxidation can consume up to 90 % of the dissolved CH_4 (Utsumi et al.



73 1998a; Kankaala et al. 2006), whereas in the well-mixed estuaries, CH₄ oxidation is believed to be
74 much less efficient (Abril et al. 2007). The CH₄ that escapes from microbial oxidation partially emits
75 from estuary across water - atmosphere interface and remaining exports to adjacent continental shelves
76 region.

77 The emitted CH₄ from sediment – atmosphere and water – atmosphere interfaces of the mangrove
78 ecosystem enrich the atmospheric CH₄ mixing ratio at a regional level (Mukhopadhyay et al. 2002) and
79 further participates in complex atmospheric CH₄ cycle. In the mangrove forest environment, emitted
80 CH₄ partially exchanges across biosphere - atmosphere interface depending upon micrometeorological
81 conditions; while the major fraction undergoes photo-oxidation depending upon ambient NO_x level. A
82 schematic diagram of atmospheric CH₄ photo-oxidation with/without NO_x concentration is presented in
83 Fig.1 (modified from Wayne, 1991).

84 This study aimed to report production, oxidation, distribution and fluxes of CH₄ in different sub-
85 ecosystems of Sundarbans for complete understanding of CH₄ biogeochemistry in the estuarine
86 mangrove environment. Beyond this primary objective, another main objective of this study was to
87 demonstrate a comprehensive CH₄ budget for Sundarbans biosphere reserve.

88 **2. Study location:**

89 Sundarbans is the largest single block of tidal mangrove forest in the world, situated over India and
90 Bangladesh at the land ocean boundary of Ganges-Brahmaputra delta and the Bay of Bengal. This



91 extensive natural mangrove forest was inscribed as a UNESCO world heritage site and covers an area of
92 10,200 sq. km of which 4200 sq. km of reserved forest is spread over India and rest part is in
93 Bangladesh. The Indian Sundarbans Biosphere Reserve (SBR) is extended over an area of 9600 km²
94 constituted of 1800 sq km estuarine waterways and 3600 sq. km reclaimed areas along with above
95 stated mangrove reserve forest. The forest is about 140 km in length from east to west and extends
96 approximately 50 – 70 km from the southern margin of the Bay of Bengal towards the north. The Indian
97 part of the Sundarbans mangrove delta is crisscrossed by the estuarine phases of several rivers namely
98 Mooriganga, Saptamukhi, Thakuran, Matla, Bidya, Gosaba and Haribhanga forming a sprawling
99 archipelago of 102 islands out of which 54 are reclaimed for human settlement and rest are virgin. One
100 of these virgin Islands is the Lothian Island, which is situated at the buffer zone of the Sundarbans
101 Biosphere Reserve covering an area of 38 km². This island completely intertidal and occupied by thick,
102 robust and resilient mangroves trees with a mean height of < 10 m. Among the mangroves, *Avicennia*
103 *alba*, *Avicennia marina* and *Avicennia officinalis* are the dominant species, *Excoecaria agallocha* and
104 *Heritiera fomes* are thinly distributed and *Ceriops decandra* is found scattered all over the island. The
105 mangrove sediment is silty clay in nature and composed of quartzo-feldspathic minerals like quartz,
106 albite and microline. The adjacent estuarine system of the island is Saptamukhi which has no perennial
107 source of freshwater and receives significant amounts of agricultural and anthropogenic runoff
108 especially during monsoon. Climate in the study area is characterized by premonsoon (February –
109 May), south west monsoon (June – September) and north east monsoon or postmonsoon (October –



110 January). Based on the above the Lothian Island and associated Saptamukhi estuary have been chosen
111 for studying CH₄ biogeochemical cycle in the Sundarbans mangrove environment. A location map of
112 Sundarbans showing Lothian Island and Saptamukhi estuary in the subset is presented in Fig.2.

113 **3. Materials and methods:**

114 The present study was carried out during June 2010 to December 2012 to cover the seasonal variation in
115 the study area. Sediment and atmospheric samples were collected from the intertidal mangrove
116 sediment & watch tower located in the center of the Lothian Island (21° 42.58'N: 88°18'E),
117 respectively. Moreover, water samples were collected from the estuarine mixing zones of the
118 Saptamukhi estuary. The details of study design, analyzed parameters and flux calculations are
119 described in the following sections.

120 Intertidal sediment samples were collected at different locations of the mangrove forest covering upper,
121 mid and lower littoral zones with the help of stainless steel corers (diameter: 10 cm) with an mean
122 penetration depth of 25 cm. Sediment cores were sectioned at 5 cm interval and collected in zipper bags
123 for transporting to the laboratory. Surface sediment temperature was measured in-situ using
124 thermometer. Simultaneously estuarine bottom sediment (sub-tidal) was also collected using grab
125 samplers. CH₄ production was measured by anaerobic incubations of sediment samples. A small portion
126 of sample (about 10 g) were weighed and taken in an incubation bottle (1.2 cm i.d. and 10 cm long)
127 fitted with rubber septum. Then the bottles were flushed with pure N₂ for 1 min to create a completely



128 anaerobic condition. The incubation was carried out in duplicate at ambient temperature for 24 hrs. At
129 the end of incubation 1 ml gas sample was withdrawn from the headspace through the rubber stopper
130 using a gas-tight glass syringe (Lu et al. 1999). CH₄ accumulation in the headspace was determined by
131 gas chromatography (Varian CP3800 GC) fitted with chrompack capillary column (12.5 m x 0.53 mm)
132 and a flame ionization detector (FID) having a mean relative uncertainty of ± 2.9 % with reference to
133 the purity of nitrogen for CH₄ as blank. CH₄ production was calculated according to CH₄ accumulation
134 in the headspace, the headspace volume and volume of samples.

135 Wet sediment samples (both intertidal and sub-tidal) are processed for measurement of CH₄
136 concentration according to Knab et al. 2009 followed by measurement of headspace for CH₄ by gas
137 chromatography as described above. The nitrate, nitrite and ammonia concentrations of the sediment
138 samples were measured taking 2M KCl extract of sediment followed by standard spectrophotometric
139 method (Grasshoff 1983). CH₄ oxidation was measured for intertidal surface sediment only, following
140 incubation with CH₄ spiked air. A fixed volume of surface sediment (~6 ml) was taken in 60 ml flasks
141 fitted with rubber septum and head space air (21% O₂) was spiked with 100 μL CH₄ L⁻¹ (10 ppmv CH₄,
142 procured from Chemtron Science Laboratories Pvt. Ltd.). These flasks were incubated in duplicate at
143 ambient temperature for 4 days. Gas samples from the head-space was drawn immediately at the onset
144 of incubation and at 24 hours interval till the end for analyzing CH₄ concentration using gas
145 chromatograph as described earlier. CH₄ oxidation was calculated according to decrease of CH₄
146 concentration in the headspace, the headspace volume and volume of sediment samples.



147 During low tide condition CH_4 emission from the intertidal sediment surface to the atmosphere was
148 measured using static Perspex chamber method (Purvaja et al. 2004). The chambers were placed in the
149 sediment for a particular duration and CH_4 emission rate was calculated based on the enrichment of CH_4
150 mixing ratio inside the chamber in comparison to the ambient air. Mixing ratio of CH_4 was measured by
151 gas chromatography as described earlier. Advective CH_4 fluxes from intertidal forest sediment to the
152 estuarine water column (F_{ISW}) were computed as (Reay et al. 1995): $F_{\text{ISW}} = \Phi \times v \times C$; where, $\Phi =$
153 porosity of sediment = 0.58 (Dutta et al. 2013), $v =$ mean linear velocity = $d\Phi^{-1}$ ($d =$ specific discharge),
154 $C =$ pore water CH_4 concentration in intertidal sediment. The specific discharge for the intertidal
155 sediment was recorded by measuring the rate of accumulation of pore water in an excavated pit of
156 known surface area (Dutta et al. 2015b). This was done during low tide condition in the intertidal flat at
157 100 m intervals along with receding water level. Diffusive CH_4 flux from sub-tidal sediment to estuary
158 was calculated using Fick's law of diffusion (Sansone et al. 2004).

159 Collection and analysis of dissolved CH_4 concentration using gas chromatograph for estuarine water has
160 been described elsewhere (Dutta et al. 2013). For measurement of CH_4 oxidation water was filled in pre-
161 cleaned (acid washed and sterilized) septum fitted incubation bottles (in a batch of 12 bottles) from
162 Niskin samplers with gentle overflowing and sealed with no air bubbles. Immediately after collection
163 two bottles are poisoned with HgCl_2 to stop microbial CH_4 oxidation and they are considered as control
164 for the experiment. Rest of the bottles are kept for incubation in ambient condition with two bottles
165 withdrawn from incubation daily and were poisoned with saturated HgCl_2 solution to continue the



166 incubation experiment up to a times series of 5 days. The concentrations of dissolved CH₄ in all
167 incubated samples was measured to record a time series kinetics of CH₄ oxidation. From the time series
168 plot, the specific rate of CH₄ oxidation was calculated by linear regression of the natural log of CH₄
169 concentration against time. The value of specific rate of CH₄ oxidation is equivalent to the slope of the
170 regression line. Actual rates of CH₄ oxidation (CH₄ consumption rate) were calculated by the product of
171 dissolved CH₄ concentration and specific rate of CH₄ oxidation (Utsumi et al. 1998b).

172 CH₄ flux across the air - water interface was calculated according to the expression (Liss and Merlivat
173 1986): $F_{WA} = k \Delta C$; where, ΔC is the difference in concentrations ($[CH_4]_{\text{observed}} - [CH_4]_{\text{equilibrium}}$) and k is
174 the gas transfer velocity in cm hr^{-1} was calculated from wind velocity and schmidt number (Liss and
175 Merlivat 1986). A positive value denotes flux from water to the atmosphere and vice versa. Water
176 temperature and pH were recorded in situ using a thermometer and a portable pH meter (Orion Star
177 A211) with a Ross combination electrode calibrated on the NBS (US National Bureau of Standards)
178 scale (Frankignoulle and Borges 2001). Reproducibility was ± 0.005 pH units. Transparency of the
179 water column was measured with a 15 cm diameter Secchi disc. Salinity and dissolved oxygen
180 concentrations in surface and bottom waters were measured onboard, following the Mohr-Knudsen and
181 Winkler titration methods, respectively (Grasshoff et al. 1983). For estimating of nitrite, nitrate and
182 ammonia concentrations samples were collected in 1L HDPE bottles and stored on ice during
183 transportation to the laboratory. In the laboratory concentrations were measured using standard
184 spectrophotometric method (Grasshoff et al. 1983) and the values were added to compute dissolved



185 inorganic nitrogen concentration (DIN). For estimating of chlorophyll concentrations samples were
186 collected in 1L amber colored bottles and stored on ice during transportation to the laboratory. In the
187 laboratory chlorophyll concentration was measured using a standard spectrophotometric method
188 (Parsons et al. 1992). Primary productivity and community respiration in the estuarine surface water
189 were measured in situ by a light and dark bottle oxygen method (Parsons et al. 1992) with a relative
190 uncertainty of $\pm 2.5\%$.

191 Samples for measurement of CH_4 mixing ratio were collected in air sampling bulbs from both 10 m and
192 20 m heights and transported to laboratory for analysis. Samples were analyzed using gas
193 chromatography (Varian CP 3800GC) fitted with chrompack capillary column (12.5 m x 0.53 mm) and
194 a flame ionization detector (FID). Two reference gas standards (10.9 ppmv and 5 ppmv, supplied by
195 Chemtron Science Laboratories Pvt. Ltd) were used before and after every measurement. Duplicate
196 samples were analyzed periodically and the replicate measurements were found to be within 2 - 3.2 %.
197 Meteorological parameters like air temperature and wind velocity were simultaneously recorded at 10
198 and 20 m heights using a portable weather monitor (Model: Davis 7440) and the value was used to
199 calculated micrometeorological indices like friction velocity (U^*), roughness height (Z_o), drag
200 coefficient and planetary boundary layer height (Ganguly et al. 2008). Biosphere - atmosphere CH_4
201 exchange flux (F_{BA}) was calculated using the following relation (Barrett 1998; Ganguly et al. 2008):

$$202 \quad F_{\text{BA}} = V_C \Delta\chi.$$



203 Where, $\Delta\chi$ = difference of mixing ratio of CH_4 between 10 and 20 m height. V_C = exchange velocity
204 which is defined as $1 / (r_a + r_s)$ (r_a = aerodynamic resistance and r_s = surface layer resistance). Negative
205 flux indicates net transfer from the atmosphere to the biosphere and positive flux indicates emission.
206 CH_4 photo-oxidation rate (P) in the lower mangrove forest atmosphere was calculated based on the
207 reaction ($\text{CH}_4 + \text{OH} \rightarrow \text{CH}_3 + \text{H}_2\text{O}$) as: $P = k [\text{CH}_4] [\text{OH}]$; where, k = rate constant of the reaction
208 between CH_4 and $\text{OH} = 1.59 \times 10^{-20} T^{2.84} \exp(-978 / T) \text{ cm}^3 \text{ molecule}^{-1} \text{ s}^{-1}$ (Vaghjiani and Ravishankara
209 1991). $[\text{CH}_4]$ = mean of all CH_4 mixing ratio measurements during the day time at 10 m height in the
210 diurnal cycle and $[\text{OH}]$ = mean of all OH radical concentrations during the day time at 10 m height in
211 the diurnal cycle in molecules cm^{-3} . OH radical concentration was computed using photolysis frequency
212 of O_3 based on the empirical relation proposed by Ehhalt and Rohrer, 2000.

213 **4. Results and discussion:**

214 **4.1 CH_4 cycling in the mangrove sediment:**

215 Mean CH_4 production potential of 20 - 25 cm deep sediment layer of the mangrove forest was 5831
216 $\mu\text{mol m}^{-3} \text{ d}^{-1}$ which is about 7.9 times higher than production potential measured for 5 – 10 cm depth
217 (table 1). Surface layer (0 – 5 cm) CH_4 production potential was not measured at the study point,
218 considering diminutive methanogenic and immense methanotrophic activity in that layer. The profile
219 could not cover up to the end of the methanogenic sediment layer, but the value clearly indicates
220 enormous CH_4 production potential of the mangrove system with a mean of $3547 \mu\text{mol m}^{-3} \text{ d}^{-1}$. The



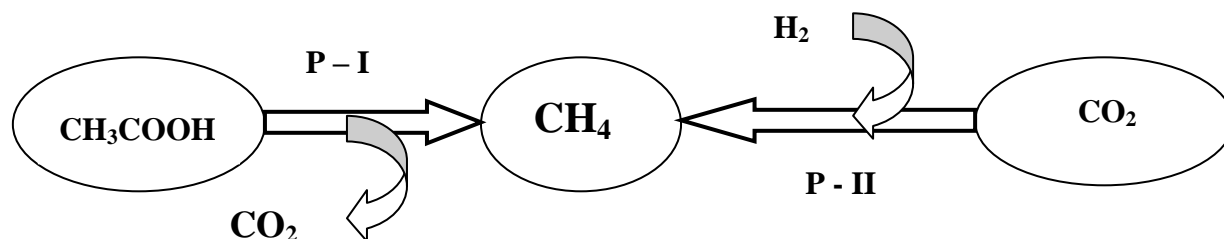
221 production potentials measured for this tropical mangrove forest sediment were within the range of that
222 reported for pristine mangrove forest at Balandra, Mexico (Strangmann et al. 2008). On seasonal basis,
223 highest production potential ($4616 \pm 2666 \mu\text{mol m}^{-3} \text{d}^{-1}$) was noticed during postmonsoon and lowest
224 ($2378 \pm 1799 \mu\text{mol m}^{-3} \text{d}^{-1}$) during premonsoon periods. The peak postmonsoon CH_4 production
225 potential may be attributed to maximum mangrove litter fall ($58.79 \text{ gm dry wt C m}^{-2} \text{ month}^{-1}$; Ray et al.
226 2011) mediated supply of organic matter in the inter-tidal sediment and subsequently inducing higher
227 CH_4 production. In contrast, high premonsoon salinity regime of the ecosystem may partially inhibited
228 CH_4 production potential of the system by supplying higher SO_4^{2-} and subsequent enhanced SO_4^{2-}
229 reduction during this phase (Dutta et al. 2015b). Geochemistry of the mangrove sediment related to this
230 study is briefly discussed elsewhere (Dutta et al. 2013) but a general trend is presented in Fig.3. The
231 Fig.3A indicates in this inter-tidal mangrove sediment requisite redox condition for the process of
232 methanogenesis ($<150 \text{ mV}$; Wang et al. 1993) is attained at $\approx 10 - 25 \text{ cm}$ depth while the process of
233 SO_4^{2-} reduction was prominent in the upper 20 cm sediment (Fig.3B). The decreasing trend of %OC
234 across deep mangrove sediment indicates significant OC mineralization by anaerobic microbial
235 metabolism (Fig.3C).

236 CH_4 production potential of first 5 cm deep sub-tidal sediment layer varied between $18.72 - 85.74 \mu\text{mol}$
237 $\text{m}^{-3} \text{d}^{-1}$ having maximal ($77.06 \pm 12.27 \mu\text{mol m}^{-3} \text{d}^{-1}$) postmonsoon and minimal ($21.28 \pm 3.63 \mu\text{mol m}^{-3}$
238 d^{-1}) premonsoon. Mean methanogenesis rate of sub-tidal sediment (0 – 5 cm) was $48.88 \pm 26.04 \mu\text{mol}$
239 $\text{m}^{-3} \text{d}^{-1}$. %OC of sub-tidal sediment surface ranged from 1.56 ± 0.72 to 2.21 ± 0.69 having maximum



240 concentration during postmonsoon and minimum during premonsoon period. About 35.25 % higher OC
241 supply in sub-tidal surface layer during postmonsoon period compare to premonsoon might have caused
242 strong redox condition favoring a higher rate of CH₄ production.

243 The %OC underwent anaerobic transformation in the 5 - 10, 10 - 15, 15 - 20 and 20 - 25 cm depths
244 were 12.7%, 9.94%, 7.64% and 8.23%, respectively. Methanogens utilize a limited number of substrates
245 and the major pathways are through fermentation of acetate (acetoclastic) and reduction of CO₂ with H₂
246 (hydrogenotrophic). The pathways for both types of methanogenesis are as follows:



249 **P - I = Acetoclastic methanogenesis; P - II = Hydrogenotrophic methanogenesis**

250 Among these two, in high CO₂ rich environment acetoclastic methanogenesis is predominant over
251 hydrogenotrophic one and approximately 70% of biologically produced CH₄ originates from conversion
252 of the methyl group of acetate to CH₄ (Mayumi et al. 2013). Based on the above fact in the intertidal
253 mangrove sediment up to the depth of penetration 25 cm, acetoclastic methanogenesis mediated OC
254 utilization rate was 59.58 mg m⁻³ d⁻¹ resulting 2483 μmol m⁻³ d⁻¹ of CH₄. The estuarine bottom sediment
255 was also OC as well as CO₂ rich and 0.82 mg m⁻³ d⁻¹ of OC transformed through acetoclastic
256 methanogenesis producing 34.22 μmol m⁻³ d⁻¹ of CH₄. Extrapolating the values for entire Sundarbans, it



257 is estimated that in the Sundarbans mangrove sediment (both inter and sub tidal sediments) about 22.86
258 Ggyr⁻¹ of OC was transformed through methanogenic pathway resulting 15.25 Ggyr⁻¹ of CH₄. The
259 mechanism also produces another radiatively active trace gas (CO₂) as a by-product of CH₄ production
260 & acetoclastic methanogenesis mediated CO₂ production rate of this mangrove forest sediment was
261 109.23 mg m⁻³ d⁻¹.

262 A major part of sedimentary produced CH₄ dissolves in the pore water at in situ high pressure resulting
263 significant super saturation (Dutta et al. 2013). Pore water CH₄ concentrations along intertidal forest
264 sediment depth profile are presented in table 1 indicating almost constant concentration up to 10 - 15 cm
265 sediment layer which abruptly increase 1.79 times at 15 - 20 cm depth and further increase to 2.26 –
266 2.76 times at 20 - 25 cm depth. On annual basis intertidal sediment pore water CH₄ concentrations
267 ranged between 3204 ± 1325 to 3639 ± 1949 nM, being maximal postmonsoon and minimal
268 premonsoon periods (Dutta et al., 2015b).

269 Statistical analysis (using MINITAB version 17) was performed between pore water CH₄ concentration
270 ([CH₄]_{PW}) vs. E_h, NO₂⁻, SO₄²⁻, AVS and organic carbon percentage (%OC) in order to point out key
271 controlling factor for variability of pore water CH₄ concentration in intertidal sediment. Here the
272 dependent variable is [CH₄]_{PW} and independent variables are E_h, NO₂⁻, SO₄²⁻, AVS and % OC. The
273 regression equation between dependent and independent variables are as follows: [CH₄]_{PW} = 10.6 -
274 0.0184 E_h - 0.123 NO₂⁻ - 0.0076 SO₄²⁻ - 0.0693 AVS - 4.09 %OC (R² = 86.6%, F = 7.79, p = 0.004, n =



275 30). From the statistical analysis (table 2) it was found that $[\text{CH}_4]_{\text{PW}}$ was significantly correlated with
276 %OC ($p = 0.004$) and E_h ($p = 0.013$) of sediment, indicating cumulative influence of %OC and E_h on
277 variability of $[\text{CH}_4]_{\text{PW}}$ in this tropical mangrove forest.

278 Following same seasonal trend annual mean pore water CH_4 concentrations in estuarine bottom lying
279 sediment varied between 2770 ± 1039 to 3980 ± 1227 nM (Dutta et al., 2015b). Compare to the adjacent
280 estuarine water (will be discussed in section 4.2) sediment pore water was 53.4 times CH_4
281 supersaturated; induces significant CH_4 influx from intertidal & sub-tidal sediment to estuary.
282 Advective CH_4 fluxes from intertidal sediment to adjacent estuary were between 115.81 ± 31.02 and
283 199.15 ± 47.89 $\mu\text{mol m}^{-2} \text{d}^{-1}$, having maximal postmonsoon and minimal premonsoon periods (Dutta et
284 al., 2015b) (Fig.4). The peak postmonsoon advective CH_4 flux may be ascribed to higher pore water
285 CH_4 concentration as well as specific discharge ($0.008 \text{ cm min}^{-1}$). Diffusive CH_4 fluxes from estuarine
286 bottom lying sediment to the water column ranged from 7.06 ± 1.95 to 10.26 ± 2.43 $\mu\text{mol m}^{-2} \text{d}^{-1}$
287 (Fig.4), having an annual mean of 8.45 $\mu\text{mol m}^{-2} \text{d}^{-1}$ (Dutta et al., 2015b). The diffusive fluxes
288 calculated for this ecosystem were comparatively higher than Yantze estuary ($1.7 - 2.2$ $\mu\text{mol m}^{-2} \text{d}^{-1}$)
289 (Zhang et al. 2008b) but much lower than White Oak river estuary (17.1 $\text{mmol m}^{-2} \text{d}^{-1}$) (Kelly et al.
290 1990). Fluxes were maximal during postmonsoon and minimal during pre-monsoon periods. The peak
291 postmonsoon diffusive CH_4 fluxes may be ascribed to maximal pore water CH_4 concentrations while the
292 reverse case applies premonsoon.



293 From the methanogenic deep sediment layer the produced CH₄ partially diffuses upward, which
294 undergoes aerobic and anaerobic oxidation in sediment before being transported to the forest
295 atmosphere. But only aerobic CH₄ oxidation at sediment surface has been included in this study. The
296 seasonal variation of surface sediment CH₄ oxidation potentials are presented in Fig.5 and the values
297 were within the range of that reported for deciduous forest of UK and temperate forests soil in Korea
298 (Bradford et al. 2001b; Jang et al. 2006). On seasonal basis, the oxidation potential was maximal
299 premonsoon and minimal monsoon periods having a mean of $1.758 \pm 0.34 \text{ mg m}^{-2} \text{ d}^{-1}$. The peak
300 premonsoon CH₄ oxidation potential may be due to maximum soil surface temperature (table 1) as
301 methanotrophy is a microbiological process and rate of any microbiological reaction is directly
302 proportional with temperature. NH₄⁺ and NO₃⁻ concentrations in mangrove forest sediment surface
303 varied between 1.01 – 3.31 μM and 1.11 – 2.98 μM, respectively and correlation between NH₄⁺ and
304 NO₃⁻ concentrations vs. CH₄ oxidation potential ($[\text{CH}_4]_{(\text{Ox})} = 1.63 - 0.307 [\text{NH}_4^+] + 0.293 [\text{NO}_3^-]$ [$R^2 =$
305 68 %, $F = 3.18$, $p = 0.181$, $n = 15$]) revealed negative relationship between $[\text{CH}_4]_{(\text{Ox})}$ and $[\text{NH}_4^+]$ but
306 positive with $[\text{NO}_3^-]$ (table 3). The inhibitory effect of $[\text{NH}_4^+]$ on CH₄ oxidation activity may be due to
307 competition of NH₄⁺ with CH₄ for the CH₄ monooxygenases (MMO) in methanotrophic bacteria. Even
308 though the affinity of MMO for CH₄ is 600 - to 1300 - fold higher than its affinity for ammonium, high
309 concentrations of ammonium are known to substantially inhibit the process of methanotrophy in
310 sediment (Be´dard and Knowles, 1989). Proportional relationship between NO₃⁻ and CH₄ oxidation may
311 be related to the demand of type II methanotrophic bacteria for nitrogen sources (Jang et al., 2006).



312 After oxidation the residual diffused CH₄ emits across sediment – atmosphere interface. Monthly
313 variation of mangrove sediment – atmosphere CH₄ exchange fluxes are presented in Fig.6; having
314 maximal emission during monsoon and minimal during premonsoon (Dutta et al. 2013). Emission
315 fluxes estimated for this study point were within the range of that reported for Pichavarm mangrove,
316 India and mangrove along the south west coast of Puerto Rico (Purvaja et al. 2004; Sotomayor et al.
317 1994). Mean soil CH₄ emission from this mangrove ecosystem was 7.06 mg m⁻² d⁻¹; indicates the
318 mangrove sediment acts as a rich source of CH₄ to the regional atmosphere. During the observation
319 period soil temperature (t) ranged between 18.25 ± 0.22 and 28.36 ± 1.02°C and variability of soil CH₄
320 emissions (E_M) were tested statistically with respective ‘t’ and pore water salinity (s). E_M is best fitted
321 linearly with ‘t’ and by a second order polynomial equation with ‘s’ as given below:

$$322 \quad E_M = 0.066 t - 1.79 \quad (R^2 = 0.35, F = 5.33, p = 0.041, n = 12)$$

$$323 \quad E_M = 0.0039 s^2 - 0.2006 s + 2.8416 \quad (R^2 = 0.77, F = 7.71, p = 0.029, n = 12)$$

324 The analysis indicates significant correlation between CH₄ fluxes with both the independent variables,
325 indicating cumulative influences of ‘t’ and ‘s’ on mangrove soil CH₄ emission. Similar phenomenon
326 was previously reported in Ranong Province mangrove area, Thailand (Lekphet et al. 2005) and a salt
327 marsh of Queen’s creek (Bartlett et al. 1987). Comparing CH₄ emissions from different littoral zones of
328 the mangrove forest, higher emissions (0.288 - 0.507 mg m⁻² hr⁻¹) were noticed from upper littoral zone
329 compare to mid & lower littoral zones; may be due to the higher pneumatophore density in that region
330 (42 number m⁻²) and diffusion of CH₄ through it (Dutta et al. 2013). Mean pneumatophore and



331 bioturbation density in the forest area was counted as 45 ± 7 and 12 ± 2 nos. m^{-2} , respectively and
332 statistical analysis was done in order to examine the influence of pneumatophore and bioturbation on
333 emission of CH_4 in this mangrove forest atmosphere. Regression equations between soil CH_4 emission
334 rate (F_{SA}) vs. pneumatophores (P_{no}) and bioturbation (B_{no}) density were as follows:

335
$$F_{\text{SA}} = - 8.59 + 0.330 P_{\text{no}} \text{ (R}^2 = 81.9\%, \text{ F} = 6.94, \text{ p} = 0.032, \text{ n} = 20)$$

336
$$F_{\text{SA}} = 6.42 - 0.052 B_{\text{no}} \text{ (R}^2 = 61.9\%, \text{ F} = 5.94, \text{ p} = 0.041, \text{ n} = 20)$$

337 The statistical analysis revealed significant correlation between dependent & independent variables for
338 both cases indicating other than physicochemical factors, biological variables (like presence of
339 pneumatophore and bioturbation) also play a crucial role for CH_4 emission from the forest sediment.
340 The positive correlation between sediment CH_4 emission rate and pneumatophore density indicates
341 plant mediated emission of CH_4 in Sundarbans mangrove ecosystem whereas negative correlation with
342 bioturbation density indicates that burrows favored sediment oxygenation especially in surface layer,
343 resulting CH_4 oxidation in surface mangrove sediment and ultimately reduced its emission flux from
344 sediment. A similar observation on oxidation of surface sediment by crab burrows in the mangrove
345 environment was previously reported by Kristensen and Alongi, 2006.

346 **4.2 Estuarine CH_4 cycling:**



347 Physicochemical and biological parameters of the estuarine water column are presented in table – 4 and
348 on monthly basis from Fig.7A to 7D. For both (temperature and salinity) the values were highest during
349 the premonsoon and lowest during the postmonsoon (for temperature) and monsoon (for salinity)
350 months. Marginal variation of temperature and salinity in estuarine surface and bottom water clearly
351 indicates a vertically well mixed water column. Surface water pH varied over a narrow range ($8.10 \pm$
352 0.03 to 8.17 ± 0.16) and seasonal differences were not significant. Dissolved oxygen (DO)
353 concentrations in estuarine surface and bottom waters were high (6.04 ± 0.73 to 7.27 ± 1.14 mg L⁻¹ and
354 5.41 ± 0.03 to 5.98 ± 0.79 mg L⁻¹, respectively) being maximal during postmonsoon and minimal during
355 monsoon periods. DO % of saturation varied between 94.8 and 99.3; indicates a well oxygenated water
356 column that would inhibit the anaerobic microbial metabolism of organic matter within estuarine water
357 column. The chlorophyll concentration in estuarine surface water ranged from 3.11 ± 0.39 to $7.88 \pm$
358 1.90 µg L⁻¹ having highest and lowest concentrations during postmonsoon and monsoon, respectively.
359 Seasonal trends of chlorophyll concentration mirrored the changes in Secchi disc depth, which ranged
360 between 29.7 ± 7.8 and 75.9 ± 7.7 cm during the study period. The ratio between primary productivity
361 and community respiration was <1, indicates the estuary is net heterotrophic in nature.

362 During the observation period estuarine surface and bottom waters dissolved CH₄ concentrations ranged
363 from 54.20 ± 5.06 to 90.91 ± 21.20 and 47.28 ± 12.85 to 67.97 ± 33.12 nM, respectively (Fig.7E);
364 having maximal postmonsoon and minimal monsoon periods (table 4) (Dutta et al., 2015b). The CH₄
365 concentrations measured in this mangrove dominated estuary was within the range of that measured in



366 Thames estuary, Loire estuary but higher than Hooghly estuary, Yangtze River estuary, Sado estuary
367 and Elbe estuary (Middelburg et al. 2002; Biswas et al. 2007; Zhang et al. 2008b). The peak
368 postmonsoon CH₄ concentrations may be attributed to cumulative effect of maximal supply of dissolved
369 CH₄ rich pore water from intertidal mangrove sediment and minimal CH₄ oxidation (will be discussed
370 later) in the estuarine water column. Like other tropical, sub-tropical and temperate estuaries (Upstill-
371 Goddard et al. 2000; Middelburg et al. 2002; Biswas et al. 2007; Zhang et al. 2008b) statistical analysis
372 revealed significant negative correlation between estuarine dissolved CH₄ levels with respective salinity
373 (Premonsoon: $R^2 = 89.1\%$, $F = 49.15$, $p < 0.001$, $n = 8$; Monsoon: $R^2 = 95.2\%$, $F = 120.12$, $p < 0.001$, n
374 $= 8$; Postmonsoon: $R^2 = 75.8\%$, $F = 18.83$, $p = 0.005$, $n = 8$) indicating salinity is the major controlling
375 factor for variability of CH₄ levels in this estuary. Moreover, the stronger degree of correlation during
376 monsoon months compare to others indicates fresh water runoff mediated addition of CH₄ to the estuary
377 during this period. Other than salinity, statistically no significant correlation was obtained with other
378 physicochemical and biological variables ($[CH_4] = -297 - 0.14 \text{ temperature} + 58 \text{ pH} + 2.69$
379 $[\text{chlorophyll}] - 19.1 [\text{dissolved oxygen}] + 8.5 (\text{NPP/R})$ [$R^2 = 75\%$, $F = 1.20$, $p = 0.513$, $n = 24$]) (table
380 5); pointed towards in situ methanogenesis is not occurring within this estuary and estuarine dissolved
381 CH₄ is entirely exogenous in nature (Dutta et al., 2015b).

382 Being well oxygenated, the water column presumably restrained methanogenesis but induced
383 methanotrophy. CH₄ oxidation in the subsurface water was studied based on time dependent CH₄
384 reduction in the incubated samples and during this experiment none of the samples showed time series



385 increment of CH₄ concentration i.e. net CH₄ production. Specific rate of CH₄ oxidation (0.009 ± 0.001
386 to 0.018 ± 0.001 hr⁻¹) and consumption (0.54 ± 0.12 to 1.26 ± 0.27 nmol L⁻¹ hr⁻¹) in estuarine surface
387 water was distinctly seasonal; having maximal premonsoon and minimal postmonsoon periods (Fig.7F).
388 The mean dissolved CH₄ consumption rate was 20.59 nmol L⁻¹ d⁻¹, about 8.11 times lower than rate of
389 CH₄ oxidation reported in the freshwater region of the Hudson estuary during summer (167 nmol L⁻¹ d⁻¹
390 ¹) (De Angelis and Scranton 1993). Aquatic CH₄ oxidation is a microbial process, so, the
391 physicochemical parameters like temperature (thermal), salinity (tonicity), oxygen (oxidative), DIN
392 (nutrient) and turbidity (surface) may have significant metabolic effects in this process. Moreover, other
393 biological processes like primary production and community respiration may be considered to be
394 influencing for this microbial process. Influence of salinity on dissolved CH₄ oxidation rate has been
395 reported previously by de Angelis & Scranton 1993. According to their observation in Hudson estuary,
396 high oxidation rates (4 to 167 nmol L⁻¹ d⁻¹) were found only at salinities below 6, rates at higher
397 salinities being 1 to 2 orders of magnitude lower. The value for dissolved O₂ was significantly above the
398 range of the estimated half-saturation constant for CH₄ oxidation, K_m (0.5 - 0.8 mg L⁻¹; Lidstrom and
399 Somers 1984) or the reported optimum range of 0.1-1.0 mg L⁻¹ (Rudd and Hamilton 1975) for microbial
400 CH₄ oxidation in the water column. Influences of dissolved inorganic nitrogen (DIN) concentration on
401 microbial CH₄ oxidation had been reported previously in Lake 227 (Rudd and Hamilton 1979).
402 According to their observation in the presence of O₂ concentrations > 31 μM bacterial CH₄ oxidation
403 was inhibited when DIN concentration was low (< 3 μM) as methanotrophs can fix nitrogen under low



404 DIN conditions ($< 3\mu\text{M}$). The nitrogen fixation is disrupted by high concentrations of O_2 but not
405 inhibited when DIN concentration reaches to $20\ \mu\text{M}$. Moreover, turbid condition of the estuary
406 methanotrophs associated with particulate matter can encounter high dissolved CH_4 levels in estuarine
407 water column (Abil et al. 2007).

408 A multiple regression analysis was done in order to point out key controlling factor for CH_4 oxidation in
409 this mangrove dominated estuary. Here the dependent variable is dissolved CH_4 oxidation rate
410 ($[\text{CH}_4]_{\text{DOX}}$) and independent variables are water temperature (T), salinity (S), dissolved oxygen (DO),
411 dissolved inorganic nitrogen (DIN), net heterotrophy (R/P) and secchi disc depth (S_d). The resultant
412 regression equation between these variables ($[\text{CH}_4]_{\text{DOX}} = -65.9 + 0.756 T - 2.18 S + 7.53 \text{ DO} - 0.408$
413 $\text{DIN} - 2.01 \text{ P/R} - 0.304 S_d$ [$R^2 = 91.6\%$, $F = 9.12$, $p = 0.014$, $n = 12$]) revealed significant correlation
414 between $[\text{CH}_4]_{\text{DOX}}$ with S, DO & S_d (table 6); indicating cumulative influence of these variables on
415 variability of $[\text{CH}_4]_{\text{DOX}}$ in this estuarine water.

416 In a study of CH_4 oxidation in a freshwater lake, Panganiban et al. 1979 reported that 30-60% of the
417 CH_4 oxidized was incorporated with the cell under aerobic conditions but essentially none was
418 incorporated under anaerobic conditions. Rudd and Taylor, 1980 reported an incorporation percentage
419 of 50% in a study of CH_4 oxidation in a freshwater lake. In the mangrove dominated estuary of
420 Sundarbans, the CH_4 oxidation in the water column progressed at aerobic conditions. Assuming that 30-
421 50% of the CH_4 carbon oxidized by methanotrophs was converted to organic matter (bacterial cell
422 materials) and the remainder to CO_2 . The mean CH_4 carbon converted to bacterial cell material was



423 computed as $0.59 \text{ mg C m}^{-2} \text{ d}^{-1}$ while primary productivity mediated production of organic carbon was
424 $1545 \text{ mg C m}^{-2} \text{ d}^{-1}$. Thus, the production of organic carbon as a result of CH_4 oxidation was only
425 0.038% of that generated by primary production at that time. The remaining oxidised CH_4 is
426 quantitatively converted to less radiatively active CO_2 & plays a crucial role in the estuarine carbon
427 cycle. Using the stoichiometric equation for aerobic CH_4 oxidation mechanism, CH_4 oxidation mediated
428 CO_2 production rate in this mangrove dominated estuary was $3.25 \text{ mg m}^{-2} \text{ d}^{-1}$. Extrapolating the value
429 for entire Sundarbans estuaries, total CO_2 production from CH_4 oxidation mechanism was 2.13 Gg yr^{-1} .

430 Surface water CH_4 % of saturation was ranged from 2483.02 ± 950.18 to 3525.45 ± 1053.72 ; indicating
431 the estuarine water was CH_4 supersaturated inducing CH_4 exchange across water – atmosphere
432 interface. Monthly variation of air – water CH_4 flux and CH_4 concentration in estuarine surface water
433 are presented graphically in Fig.7E. Air – water CH_4 fluxes from this estuary ranged between $6.27 \pm$
434 1.61 and $10.67 \pm 6.92 \text{ } \mu\text{mol m}^{-2} \text{ d}^{-1}$; having minimal premonsoon and maximal monsoon periods (Dutta
435 et al., 2015b). Minimal premonsoon CH_4 fluxes may be attributed to the lowest value of wind speed
436 over the estuary as well as surface water dissolved CH_4 levels. Flux values estimate for this site fall
437 within the range measured in the Hooghly estuary ($0.88 - 148.63 \text{ } \mu\text{mol m}^{-2} \text{ d}^{-1}$) (Biswas et al. 2007) but
438 are much lower than those reported for some other estuaries like Oregon estuary ($181.3 \text{ } \mu\text{mol m}^{-2} \text{ d}^{-1}$)
439 (De Angelis and Lilley, 1987). The large variation in water – atmosphere CH_4 flux between different
440 estuaries reflects a combination of dissolved CH_4 concentration, the gas transfer velocity and variability
441 of estuarine regimes (Dutta et al., 2015b). Wind speed over the estuarine water surface ranged between



442 2.28 ± 1.01 and $3.16 \pm 1.79 \text{ ms}^{-1}$. The value seems to be low; may be due to high resistance offered by
443 the mangrove vegetation resulting low gas transfer velocity as well as air - water CH_4 exchange flux
444 value in this estuary. Our flux estimates were analyzed statistically to examine the influence of
445 temperature and salinity on their variability. In both cases the analysis revealed significant correlations
446 (water temperature: $R^2 = 61\%$, $F = 6.71$, $p = 0.029$, $n = 24$; salinity: $R^2 = 54\%$, $F = 5.31$, $p = 0.037$, $n =$
447 24) indicating a cumulative effect of temperature and salinity on estuarine CH_4 emission (Dutta et al.,
448 2015b).

449 **4.3. Atmospheric CH_4 dynamics:**

450 Temperature of the mangrove forest atmosphere varied between 17.34 ± 4.0 to $30.34 \pm 0.91^\circ\text{C}$ at 10 m
451 and 16.17 ± 1.80 to $29.73 \pm 1.13^\circ\text{C}$ at 20 m; being maximal premonsoon and minimal postmonsoon
452 seasons (table 7). Wind velocity varied between 0.41 ± 0.36 and $1.32 \pm 1.11 \text{ m s}^{-1}$ at 10 m height and
453 0.80 ± 0.88 to $1.64 \pm 1.37 \text{ m s}^{-1}$ at 20 m height; having maximal monsoon and minimal postmonsoon
454 periods. The atmospheric turbulence expressed by friction velocity (U^*) plays an important role in
455 controlling the stability of the atmosphere & varied between 0.01 and 1.2 m s^{-1} . Planetary boundary
456 layer or atmospheric boundary layer (PBL) height over the mangrove forest atmosphere varied between
457 702.45 m and 936.59 m ; having maximal height during premonsoon and minimal during monsoon
458 periods. Mean atmospheric boundary layer height over the tropical mangrove forest atmosphere was
459 811.7 m on annual basis. Values of other micrometeorological indices such as drag coefficient and



460 roughness height are presented in table 5. The seasonal variation for drag co-efficient may be attributed
461 to the variation of wind speed in this mangrove forest atmosphere (Smith and Banke, 1975) while the
462 values for both drag coefficient and roughness height were minimum in monsoon period. The low
463 values of drag coefficient and roughness length could be deemed specific for this particular surface
464 which is due to the action of low - pressure force on individual surface elements and the low shearing
465 stress generated by particular wind (Mukhopadhyay et al., 2002).

466 Monthly variation of CH₄ mixing ratio at 10 & 20 m heights of the forest atmosphere are presented in
467 Fig.8A; indicating minimal premonsoon (at both 10 and 20 m heights) and maximal during monsoon
468 and postmonsoon periods for 10 m and 20 m heights, respectively (table 7). The maximal monsoon CH₄
469 mixing ratio at 10 m height may be attributed to maximum monsoon CH₄ emission from sediment and
470 aquatic surfaces and primarily it's mixing to the lower atmosphere of the mangrove ecosystem. Diurnal
471 variation of CH₄ in the mangrove forest atmosphere at 10 m and 20 m heights in a month of January is
472 presented in Fig.8B; indicating peak concentrations during early morning may be attributed to CH₄
473 accumulation within a stable boundary layer in that period (Dutta et al., 2013c). With progress of the
474 day due to increment of atmospheric turbulence the stable layer breaks up resulting decrease of CH₄
475 concentration in the lower atmosphere (Mukhopadhyay et al. 2002). Changes in the
476 micrometeorological parameters at the study site change the stability (Z/L) of the atmosphere, which in
477 turn may alter the atmospheric CH₄ mixing ratio in the lower atmosphere ([CH₄]_{10m}). Statistical analysis
478 revealed significant correlation between Z/L and [CH₄]_{10m} ([CH₄]_{10m} = 2.56 + 2.25 Z/L [R² = 74.8%, p



479 < 0.001, $F = 29.73$, $n = 30$]); indicates potential impact of micrometeorological parameters on
480 variability of CH_4 mixing ratio at lower atmosphere. Comparing CH_4 distribution along vertical column
481 of the forest atmosphere it was evident that CH_4 mixing ratio at 10 m height was 1.02 times higher than
482 20 m height; induces biosphere – atmosphere CH_4 exchange in this mangrove environment depending
483 upon micrometeorological conditions of the atmosphere. Monthly variation of biosphere – atmosphere
484 CH_4 exchange flux is presented in Fig.8C having maximal flux monsoon and minimal postmonsoon
485 periods. This mangrove biosphere acts as a source for CH_4 during monsoon, when $\Delta\chi$ is significantly
486 positive and as sink during pre and post monsoon seasons, when $\Delta\chi$ is negative. The contributory
487 processes to the $\Delta\chi$ are emission from water and soil resulting enrichment in the 10 m layer and
488 oxidation (both microbial and photochemical) causing depletion at 10 and 20 m, respectively (Dutta et
489 al. 2013). Mean biosphere – atmosphere methane exchange flux was calculated as $0.086 \text{ mg m}^{-2} \text{ d}^{-1}$;
490 indicates on annual mean basis the mangrove ecosystem acts as a source of CH_4 to the upper
491 atmosphere. Mean compensation point (i.e. where net biosphere - atmosphere CH_4 flux is zero) for CH_4
492 in this subtropical mangrove forest was 1.997 ppmv. Statistical analysis was done between biosphere –
493 atmosphere CH_4 flux (F_{BA}) and sensible heat flux (H) as the transport of energy and mass are partially
494 controlled by ‘ H ’. The regression equation [$F_{\text{BA}} = - 0.0013 H^2 + 0.0967 H + 0.7789$ ($R^2 = 0.53$, $F =$
495 7.72 , $p = 0.002$, $n = 12$)] explains 53% variability between dependent & independent variables
496 indicating significant influence of sensible heat flux on variability of biosphere – atmosphere CH_4
497 exchange in this tropical mangrove forest ecosystem.



498 On annual basis mean daytime CH₄ mixing ratio was 1.03 times lower than night-time; the variability is
499 presumed to be governed by photo-oxidation and diurnal changes in the boundary layer height. But
500 statistically no significant correlation was obtained between variability of daytime and nighttime CH₄
501 mixing ratio with PBL height ($\Delta\text{CH}_4 = -0.0118\Delta\text{PBL} + 0.3045$, $R^2 = 16.2\%$, $F = 0.321$, $p = 0.987$, $n =$
502 12); indicating variability of atmospheric boundary layer height was not the major controlling factor for
503 ΔCH_4 , that pointed towards large atmospheric CH₄ photo-oxidation in the mangrove forest atmosphere.
504 CH₄ photo-oxidation rate in this subtropical mangrove forest atmosphere varied between 6.05×10^{10} and
505 1.67×10^{11} molecules $\text{cm}^{-3} \text{d}^{-1}$ being maximum oxidation during monsoon and minimum during
506 postmonsoon periods (Dutta et al. 2015c). The peak monsoon CH₄ photo-oxidation rate may be
507 attributed to maximum CH₄ supply through emission as well as high UV index and UV erythermal dose
508 irradiance during this period in these subtropical latitudes (Panicker et al. 2014). Considering the mean
509 day light period as 12 hours and 6.023×10^{23} molecules equals to 1 mole or 16000 mg CH₄, the mean
510 CH₄ photo-oxidation rate in this tropical mangrove forest atmosphere was calculated as 3.25×10^{-9} mg
511 $\text{cm}^{-3} \text{d}^{-1}$.

512 **4.4: Quantitative CH₄ budget from Indian Sundarbans:**

513 A box diagram (fig.9) was constructed for describing biogeochemical CH₄ cycling in Sundarbans
514 biosphere reserve. In the model different subsystems are designated as separate reservoir. CH₄ storage in
515 each reservoir and exchange fluxes of CH₄ between different reservoirs are presented as an annual mean



516 and values were used to calculate the input and output of CH₄ to/from the reservoirs, which in turn
517 established the CH₄ budget for this mangrove-dominated estuarine system.

518 **Mangrove sediment methane budget:**

- 519 1. Mean CH₄ production potential in intertidal forest sediment (up to the depth of 25 cm) was 3547
520 $\mu\text{mol m}^{-3} \text{d}^{-1}$. Considering the rate equal to in situ CH₄ production and extrapolating over entire
521 forest, total CH₄ production within 25 cm depth of the forest sediment is 21.75 Ggyr⁻¹.
- 522 2. Intertidal sediment pore water CH₄ concentration was 3451 nM and extrapolating the
523 concentration for entire mangrove forest (up to 25 cm depth), the sediment stands as a reservoir
524 pool of 0.031Gg CH₄.
- 525 3. The intertidal sediment pore water methane concentration was about 55 times supersaturated
526 than adjacent estuarine water (63.04 nM) indicating significant out - flux of CH₄ rich pore water
527 from intertidal sediment to estuary during low tide phase via advective transport.
- 528 4. About 8.2% of the produced CH₄ is advectively transported to the adjacent estuarine system with
529 a rate of 159.52 $\mu\text{mol m}^{-2} \text{d}^{-1}$.
- 530 5. Mean CH₄ oxidation potential at intertidal forest sediment surface was 1.758 mg m⁻² d⁻¹ and
531 total oxidation was 2.70 Ggyr⁻¹, when extrapolated for entire forest area of Sundarbans. The



532 value indicates only 12.41% of produced CH_4 is oxidized at sediment surface; presenting petite
533 activity of methanotrophs in comparison to the methanogens in forest sediment.

534 6. Total CH_4 emission across sediment – atmosphere interface of the mangrove forest was 10.8
535 Ggyr^{-1} (about 49.6% of total produced CH_4 in sediment) with a rate of $7.06 \text{ mg m}^{-2} \text{ d}^{-1}$.

536 7. The total CH_4 emission and oxidation from/at the mangrove surface sediment was 6.05 and 1.51
537 times higher, respectively compare to total CH_4 advectively transported to the estuary; indicates
538 emission acts as major CH_4 removal pathway from intertidal mangrove sediment.

539 8. Balancing total production and removal, annually 6.46 GgCH_4 remains unexplained. This
540 establishes the existence of anaerobic methane oxidation in mangrove sediment column which
541 was not covered in this study.

542 **Sub-tidal sediment CH_4 budget:**

543 1. CH_4 production potential of 0 – 5 cm depth of estuarine underlying sediment (sub-tidal
544 sediment) was $48.88 \mu\text{mol m}^{-3} \text{ d}^{-1}$ and total production was 0.026 Ggyr^{-1} when extrapolated for
545 entire sub-tidal area for estuaries of Sundarbans.

546 2. Mean sub-tidal sediment (0 – 5 cm) pore water CH_4 concentration was 3286 nM; which was
547 about 52.13 times supersaturated than overlying estuarine water inducing diffusive CH_4 transport
548 from sub-tidal sediment to the overlying estuary.



549 3. Mean diffusive CH₄ flux from sub-tidal sediment to the overlying estuary was 8.45 μmol m⁻² d⁻¹.
550 Extrapolating the rate for entire sub-tidal area of Sundarbans, the sub-tidal sediment acts as a
551 source of 0.089 GgCH₄ annually to the upper estuarine system.

552 **Estuarine CH₄ budget:**

553 1. Total CH₄ input from sediment to estuary (by both advection and diffusion transports) was
554 1.875Gg yr⁻¹. Advective flux being 20 times higher than diffusive flux acts as major source for
555 CH₄ to the estuary.

556 2. Mean dissolved CH₄ concentration in the estuary was 63.04 nM. Extrapolating this over the
557 entire volume of the estuaries of the Sundarbans, the system stands as a reserve pool of 0.011Gg
558 CH₄ (Dutta et al., 2015b).

559 3. The total CH₄ oxidation rate in the estuarine water column was 1.30Ggyr⁻¹ with a rate of 20.59
560 nmol L⁻¹ d⁻¹.

561 4. Mean CH₄ emission flux across the water - atmosphere interface of the estuary was 8.88 μmol m⁻²
562 d⁻¹. Extrapolating this over the total estuarine surface area, on an annual basis the mangrove
563 associated estuaries of the Sundarbans are a source of 0.093Gg CH₄ to the regional atmosphere,
564 which is only 4.96 % of total CH₄ supplied to the estuary.



- 565 5. CH₄ oxidation, being 14 times higher than water - atmosphere exchange, is considered as
566 principal CH₄ removal mechanism in this estuary.
- 567 6. Mean turnover time of CH₄ in the water column relative to oxidation and emission was 3.77
568 days, which is in the range of turnover times relative to oxidation reported for the low salinity
569 region of the Hudson estuary (1.4 – 9 days) (De Angelis and Scranton 1993).
- 570 7. The total sink of CH₄ due to these oxidation and emission processes were 1.39 Ggyr⁻¹, about
571 74.13 % of total CH₄ supply to the estuary, indicating a significant export flux of CH₄ from
572 estuary to the adjacent continental shelf.
- 573 8. Balancing CH₄ sources vs. sinks in this estuarine system, the export flux of CH₄ from estuary to
574 the continental shelf was 0.485 Ggyr⁻¹, indicating a significant contribution from the Sundarbans
575 estuaries to the CH₄ budget of the northern Bay of Bengal (Dutta et al., 2015b).

576 **Atmospheric CH₄ budget:**

- 577 1. Net CH₄ emission from Sundarbans mangrove ecosystem (sediment & estuarine surfaces) to the
578 regional atmosphere was 10.89 Ggyr⁻¹, of which sediment is the principal contributor (99.17%).
- 579 2. Comparison to the global mean CH₄ emission rate from mangrove forest & creeks (10.76 mg m⁻²
580 d⁻¹; Barnes et al., 2006) mean CH₄ emission rate from Sundarbans mangrove environment is



581 approximately 2.99 times lower; representing partial impact of this mangrove system towards
582 earth's global warming as well as climate change scenario.

583 3. Atmospheric CH₄ mixing ratio in 10 m and 20 m heights of the forest atmosphere were 2.038
584 and 1.987 ppmv, respectively having mean of 2.013 ppmv. Extrapolating over entire Sundarbans
585 up to the height of atmospheric boundary layer (811.7 m), atmosphere stands as a reservoir pool
586 of 11.2 GgCH₄.

587 4. The annual mean mangrove biosphere atmosphere CH₄ exchange flux was 0.086 mg m⁻² d⁻¹ and
588 the former when multiplied by the total forest area of the Sundarbans yields that this tropical
589 mangrove ecosystem annually acts as source for 0.30 GgCH₄ to the regional atmosphere (about
590 2.75% of total CH₄ input from water & sediment surfaces).

591 5. Total CH₄ photo-oxidation in the forest atmosphere up to height of atmospheric boundary layer
592 was 9.26 Ggyr⁻¹ with a mean rate of 3.25 x 10⁻⁹ mg cm⁻³ d⁻¹. Compare to total CH₄ supply to the
593 forest atmosphere, about 85% is photo-oxidized within atmospheric boundary layer of
594 Sundarbans and is recognized as major atmospheric CH₄ removal pathway. The photo-oxidation
595 mediated depletion of CH₄ is highly significant in atmospheric chemistry producing byproducts
596 like HCHO, O₃ depending upon ambient NO_x level. Balancing total atmospheric sources and
597 sinks, annually 1.33Gg CH₄ remains unbalanced in the atmosphere, which enriches regional
598 atmospheric CH₄ mixing ratio.

599 **5. Conclusion:**



600 CH₄ production potential within 25 cm depth of the forest sediment is 21.75 Ggyr⁻¹ and pore water CH₄
601 concentration was 3541 nM. CH₄ fluxes across intertidal sediment – atmosphere interface acts as major
602 sink for produced CH₄ in intertidal sediment over surface layer CH₄ oxidation and advective CH₄
603 transport to estuary. The process of methanogenesis is totally restricted within estuarine water column
604 and is supplied from adjacent mangrove forest ecosystem and underlying sediment of the estuary.
605 Advective flux being 20 times higher than diffusive flux acts as major source for CH₄ to the estuary.
606 CH₄ oxidation, being 14 times higher than water - atmosphere exchange, is considered the principal
607 CH₄ removal mechanism in this estuary. Total annual CH₄ emission from sediment and water surfaces
608 of the Sundarbans mangrove biosphere was 10.89Gg, of which sediment is the principal contributor
609 (99.17%). Compare to total CH₄ supply to the atmosphere, about 85% is photo-oxidized within
610 atmospheric boundary layer of Sundarbans and 2.75% is transported to the upper atmosphere through
611 biosphere – atmosphere CH₄ exchange flux.

612 **6. Acknowledgement:**

613 The authors thank the Ministry of Earth Science, Govt. of India sponsored Sustained Indian Ocean
614 Biogeochemistry and Ecological Research (SIBER) programme for partial financial support to carry out
615 the study. We are thankful to the Sundarbans Biosphere Reserve for extending necessary help and
616 support for conducting fieldwork and measurements related to the study.

617 **7. References:**



- 618 Abril, G., Commarieu, M.V., Gue´rin, F.: Enhanced methane oxidation in an estuarine turbidity
619 maximum. *Limnol. Oceanogr.* 52(1), 470 – 475, 2007.
- 620 Barnes, J., Ramesh, R., Purvaja, R., Nirmal Rajkumar, A., Senthil Kumar, B., Krithika, K.,
621 Ravichandran, K., Uher, G., Upstill-Goddard, R.: Tidal dynamics and rainfall control N₂O and CH₄
622 emissions from a pristine mangrove creek. *Geophys. Res. Lett.* 33, L15405, 2006.
- 623 Barrett K.: Oceanic ammonia emissions in Europe and their transboundary fluxes. *Atmospheric*
624 *Environment* 32, 381 – 391, 1998.
- 625 Bartlett, K. B., Bartlett, D. S., Harris, R. C., Sebacher, D. I.: Methane emissions along a salt marsh
626 gradient. *Biogeochemistry* 4, 183-202, 1987.
- 627 Be´dard, C., Knowles, R., 1989. Physiology, biochemistry, and specific inhibitors of CH₄, NH₄⁺, and
628 CO oxidation by methanotrophs and nitrifiers. *Microbiol. Rev.* 53, 68–84.
- 629 Biswas, H., Mukhopadhyay, S.K., Sen, S., Jana, T.K.: Spatial and temporal patterns of methane
630 dynamics in the tropical mangrove dominated estuary, NE Coast of Bay of Bengal, India. . *J. Mar. Syst.*
631 68, 55–64, 2007.



- 632 Bouillon, S., Middelburg, J.J., Dehairs, F., Borges, A.V., Abril, G., Flindt, M.R., Ulomi, S., Kristensen,
633 E.: Importance of intertidal sediment processes and porewater exchange on the water column
634 biogeochemistry in a pristine mangrove creek (Ras Dege, Tanzania). *Biogeosciences* 4, 311-322, 2007c.
- 635 Bradford, M.A., Ineson, P., Wookey, P.A., Lappin-Scott, H.M.: The effects of acid nitrogen and acid
636 sulphur deposition on CH₄ oxidation in a forest soil: a laboratory study. *Soil Biol Biochem* 33,1695 –
637 1702, 2001b.
- 638 Canfield, D. E., Kristensen, E., Thamdrup, B.O.: The sulfur cycle. *Advanced Marine Biology* 48, 313 –
639 381, 2005.
- 640 De Angelis, M.A., Scranton, M.I.: Fate of methane in the Hudson River and estuary. *Glob.*
641 *Biogeochem. Cycles* 7, 509 –523, 1993.
- 642 De Angelis, M.A., Lilley, M.D.: Methane in surface waters of Oregon estuaries and rivers. *Limnol.*
643 *Oceanogr.* 32, 716 –722, 1987.
- 644 Dutta, M.K, Ray, R., Mukherjee, R., Jana, T.K., Mukhopadhyay, S.K.: Atmospheric fluxes and photo-
645 oxidation of methane in the mangrove environment of the Sundarbans, NE coast of India; A case study
646 from Lothian Island. *Agricultural and Forest Meteorology*, 213, 33 – 41, 2015c.



- 647 Dutta, M.K., Mukherkjee, R., Jana, T.K., Mukhopadhyay, S.K.: Biogeochemical dynamics of
648 exogenous methane in an estuary associated to a mangrove biosphere; the Sundarbans, NE coast of
649 India. *Marine Chemistry* 170, 1 – 10, 2015b.
- 650 Dutta, M.K., Chowdhury, C., Jana, T.K., Mukhopadhyay, S.K.: Dynamics and exchange fluxes of
651 methane in the estuarine mangrove environment of Sundarbans, NE coast of India. *Atmos. Environ.* 77,
652 631-639, 2013.
- 653 Ding, W., Cai, Z., Tsuruta, H., Li, X.: Key factors affecting spatial variation of methane emissions
654 from freshwater marshes. *Chemosphere* 51, 167–173, 2003.
- 655 Ehhalt D.H., Rohrer, F.: Dependence of the OH concentration on solar UV. *Journal of Geophysical*
656 *Research*, 105, 3565-3571, 2009.
- 657 Frankignoulle, M., Borges, A.V.: Direct and indirect pCO₂ measurements in a wide range of pCO₂ and
658 salinity values (the Scheldt estuary), *Aquat. Geochem.* 7, 267–273, 2001.
- 659 Ganguly D., Dey, M., Mandal, S.K., De, T.K., Jana, T.K.: Energy dynamics and its implication to
660 biosphere-atmosphere exchange of CO₂, H₂O and CH₄ in a tropical mangrove forest canopy.
661 *Atmospheric Environment*, 42, 4172 – 4184, 2008.
- 662 Grasshoff, K., Ehrhardt, M., Kremling, K.: *Methods of seawater analysis*, 2nd edition. Germany, 1983.



- 663 Hanson, R.S., Hanson, T.E.: Methanotrophic bacteria. *Micro. and Mole. Bio. Rev.* 60, 439-471, 1996.
- 664 Hoehler, T.M., Alperin, M.J.: Biogeochemistry: Methane minimalism. *Nature* 507, 436 – 437, 2014.
- 665 IPCC, 2007. Summary for policymakers. In: Solomon, S., et al. (Ed.), *Climate Change*
666 2007: the Physical Science Basis. Contribution of Working Group I to the Fourth Assessment
667 Report of the Intergovernmental Panel on Climate Change. Cambridge University
668 Press, Cambridge.
- 669 Jang, I., Lee, S., Hong, J., Kang, H.: Methane oxidation rates in forest soils and their controlling
670 variables: a review and a case study in Korea. *Ecol Res*, 21, 849–854, 2006.
- 671 Kankaala, P., Huotari, J., Peltomaa, E., Saloranta, T., Ojala, A.: Methanotrophic activity in relation to
672 methane efflux and total heterotrophic bacterial production in a stratified, humic, boreal lake. *Limnol.*
673 *Oceanogr.* 51, 1195–1204, 2006.
- 674 Kelley, C.A., Martens, C.S., Chanton, J.P.: Variations in sedimentary carbon remineralization rates in
675 the White Oak River estuary, North Carolina. *Limnol. Oceanogr.* 35, 372–383, 1990.
- 676 Keller, J. K., Takagi, K. K.: Solid-phase organic matter reduction regulates anaerobic decomposition in
677 bog soil. *Ecosphere*, 4, 54, 2003.



- 678 Knab, N. J., Cragg, B.A., Hornibrook, E.R.C., Holmkvist, L., Pancost, R.D., Borowski, C., Parkes, R.J.,
679 Jørgensen, B.B.: Regulation of anaerobic methane oxidation in sediments of the Black Sea.
680 *Biogeosciences*, 6, 1505–1518, 2009.
- 681 Kristensen, E., Flindt, M.R., Ulomi, S., Borges, A.V., Abril, G., Bouillon, S.: Emission of CO₂ and CH₄
682 to the atmosphere by sediments and open waters in two Tanzanian mangrove forests. *Mar. Ecol. Prog.*
683 *Ser.* 370, 53–67, 2008.
- 684 Kristensen, E., Alongi, D.M.: Control by fiddler crabs (*Uca vocans*) and plant roots (*Avicennia marina*)
685 on carbon, iron, and sulfur biogeochemistry in mangrove sediment. *Limnology and Oceanography*,
686 51(4), 1557–1571, 2006.
- 687 Lekphet, S., Nitorisavut, S., Adsavakulchai, S.: Estimating methane emissions from mangrove area in
688 Ranong Province, Thailand. *Songklanakarin J. Sci. Technol.*, 27(1), 153-163, 2005.
- 689 Lelieveld, J., Crutzen, P.J., Dentener, F.J., Changing concentration, lifetime and climate forcing of
690 atmospheric methane. *Tellus* 50B, 128–150, 1993.
- 691 Lidstrom, M. E., Somers, L.: Seasonal study of methane oxidation in Lake Washington. *Appl. Environ.*
692 *Microbiol.* 47, 1255-1260, 1984.



- 693 Liss, P.S., Merlivat, L.: Air sea gas exchange rates: introduction and synthesis. In: Buat-Menard, P.
694 (Ed.), *The Role of Air Sea Exchange in Geochemical Cycling*. D. Reidel, Hingham, MA, 113 – 129,
695 1986.
- 696 Lu, C.Y., Wong, Y.S., Tam, N.F.Y., Ye, Y., Lin, P.: Methane flux and production from sediments of a
697 mangrove wetland on Hainan Island China. *Mangroves Salt Marshes*, vol. 3, no. 1, p. 41-49, 1999.
- 698 Mayumi, D., Mochimaru, H., Yoshioka, H., Sakata, S., Maeda, H., Miyagawa, Y.: Evidence for
699 syntrophic acetate oxidation coupled to hydrogenotrophic methanogenesis in the high-temperature
700 petroleum reservoir of Yabase oil field (Japan). *Environ. Microbiol.* 13, 1995–2006, 2011.
- 701 Mukhopadhyay S.K., Biswas, H., De, T.K., Sen, S., Sen, B.K., Jana, T.K.: Impact of Sundarbans
702 mangrove biosphere on the carbon dioxide and methane mixing ratio at the NE coast of Bay of Bengal,
703 India. *Atmospheric Environment* 36 (4), 629–638, 2002.
- 704 Megonigal, J.P., Hines, M.E., Visscher, P.T.: Anaerobic metabolism: linkages to trace gases and aerobic
705 processes. In *Biogeochemistry*. Ed. W.H. Schlesinger. Elsevier-Pergamon, Oxford, 317– 424, 2004.
- 706 Middelburg, J.J., Nieuwenhuize, J., Iversen, N., Hoegh, N., DeWilde, H., Helder, W., Seifert, R.,
707 Christof, O.: Methane distribution in European tidal estuaries. *Biogeochemistry* 59, 95–119, 2002.



- 708 Panicker A.S., Pandithurai, G., Beig, G., Kim, D., Lee, D.: Aerosol modulation of ultraviolet radiation
709 dose over four metro cities in India. *Advances in Meteorology* Article ID 202868, 5 pages, 2014.
- 710 Parsons, T.R., Maita, Y., Lalli, C.M.: A manual of chemical and biological methods for sea water
711 analysis. New York, Pergamon Press, 1992.
- 712 Purvaja, R., Ramesh R., Frenzel, P.: Plant-mediated methane emission from an Indian mangrove.
713 *Global Change Biology*, 10, 1–10, 2004.
- 714 Panganiban, A. T., Patt, Jr., T. E., Hanson. R. S.: Oxidation of methane in the absence of oxygen in the
715 lake water samples. *Appl. Environ. Microbiol.* 37, 303-309, 1979.
- 716 Ray, R., Ganguly, D., Chowdhury, C., Dey, M., Das, S., Dutta, M.K., Mandal, S.K., Majumder, N., De,
717 T.K., Mukhopadhyay, S.K., Jana, T.K.: Carbon sequestration and annual increase of carbon stock in a
718 mangrove forest. *Atmospheric Environment*, 45, 5016 – 5024, 2011.
- 719 Reay, W.G., Gallagher, D., Simmons, G.M.: Sediment water column nutrient exchanges in Southern
720 Chesapeake Bay near shore environments. Virginia Water Resources Research Centre, Bulletin- 181b,
721 1995.
- 722 Rudolf, K.T., Seigo, S.: Methane and microbes. *Nature* 440, 878 – 879, 2006.
- 723 Rudd, J.W., Taylor, C.W.: Methane cycling in aquatic environments. *Adv. Aquatic Microbial.* 2, 77-
724 150, 1980.



- 725 Rudd, J. W., M., Hamilton, R.D.: Factors controlling rates of methane oxidation and the distribution of
726 the methane oxidizers in a small stratified lake. *Arch. Hydrobiol.* 75, 522- 538, 1975.
- 727 Rudd, J. W., M., Hamilton, R.D.: Methane cycling in Lake 227 in perspective with some components of
728 carbon and oxygen cycles. *Arch. Hydrobiol. Beih. Ergebn. Limnol.* 12, 115-122, 1979.
- 729 Sansone, F.J., Graham, A.W.: Methane along western Mexican margin. *Limnol. Oceanogr.* 49(6), 2242
730 – 2255, 2004.
- 731 Strangmann, A., Bashan, Y., Giani, L.: Methane in pristine and impaired mangrove soils and its
732 possible effect on establishment of mangrove seedlings. *Biology and Fertility of Soils*, vol. 44, no. 3,
733 511-519, 2008.
- 734 Sotomayor, D., Corredor, J.E., Morell, M.J.: Methane flux from mangrove sediments along the
735 southwestern coast of Puerto Rico. *Estuaries* 17 (1B), 140–147, 1994.
- 736 Smith, S.D., Banke, E.G., 1975. Variation of sea surface drag coefficient with wind speed. *Quarterly*
737 *Journal of Royal Meteorological Society*, 101, 665–673.
- 738 Utsumi, M., Nojiri, Y., Nakamura, T., Nozawa, T., Otsuki, A., Takamura, N., Watamabe, N., Seki, H.:
739 Dynamics of dissolved methane and methane oxidation in a dimictic Lake Nojiri during winter. *Limnol.*
740 *Oceanogr.* 43(1), 10-17, 1998a.



- 741 Utsumi, M., Nojiri, Y., Nakamura, T., Nozawa, T., Otsuki, A., Takamura, N., Watamabe, N., Seki, H.:
742 Oxidation of dissolved methane in eutropic shallow lake: Lake Kasumigaura, Japan. *Limnol. Oceanogr.*
743 43(3), 471-480, 1998b
- 744 Upstill-Goddard, R.C., Barnes, J., Frost, T., Punshon, S., Owens, N. J. P.: Methane in the Southern
745 North Sea: low salinity inputs, estuarine removal and atmospheric flux. *Glob. Biogeochem. Cycles*, 14,
746 1205–1217, 2000.
- 747 Vaghjiani, G.L., Ravishankara, A.R.: New measurement of the rate coefficient for the reaction of OH
748 with methane. *Nature* 350, 406 – 409, 1991.
- 749 Wang, Z.P., Delaune, R.D., Patrick Jr., W.H., Masscheleyn, P.H.: Soil redox and pH effects on methane
750 production in a flooded rice soils. *Soil Sci. Society of America Journal* 57, 382-385, 1993.
- 751 Wayne P.: "Chapter 5: The Earth's Troposphere", *Chemistry of Atmospheres, An Introduction to the*
752 *Chemistry of Atmospheres of Earth, the Planets and their Satellites*. Oxford Clarendon Press, 209 – 275,
753 1991.
- 754 Zhang, G., Zhang, J., Lui, S., Ren, J., Xu, J., Zhang, F. : Methane in the Changjiang (Yangtze River)
755 Estuary and its adjacent marine area: riverine input, sediment release and atmospheric fluxes.
756 *Biogeochemistry*, 91, 71–84, 2008b.

757



758 **Table 1: Seasonal variation of CH₄ production potential and pore water CH₄ concentrations in**
 759 **intertidal and sub-tidal sediments. Here, T = soil surface temperature; S = pore water salinity;**
 760 **[CH₄]_(PI) = CH₄ production potential in intertidal sediment; IS = intertidal sediment; SS = sub-**
 761 **tidal sediment.**

Season	T (°C)	S	Depth (cm)	[CH ₄] _(PI) (μmol m ⁻³ d ⁻¹)	[CH ₄] _(IS) (μM)	[CH ₄] _(SS) (μM)
Premonsoon	28.36 ± 1.02	28.88 ± 0.13	0 – 5	ND	2292	2770 ± 1039
			5 – 10	214.99	2313	
			10 – 15	2088.67	2334	
			15 – 20	2918.89	3804	
			20 – 25	4290.22	5274	
Monsoon	28.01 ± 0.41	22.55 ± 0.31	0 – 5	ND	1881	3110 ± 1023
			5 – 10	823.58	2155	
			10 – 15	3539.90	2429	
			15 – 20	4373.44	4508	
			20 – 25	5850.478	6587	
Postmonsoon	18.25 ± 0.22	25.98 ± 0.45	0 – 5	ND	2246	3980 ± 1227
			5 – 10	1175.56	2319	
			10 – 15	4033.30	2413	
			15 – 20	5903.10	4542	
			20 – 25	7352.94	6670	



762 **Table 2: Results of multiple regression analysis between pore water CH₄ concentrations, E_h, NO₂⁻,**
763 **SO₄²⁻, AVS and organic carbon (OC) concentration.**

Predictor	Coef	SE Coef	T	P
Constant	10.601	2.921	3.63	0.005
E_h	-0.018447	0.009074	-2.03	0.013
NO₂⁻	-0.12277	0.05477	-2.24	0.052
SO₄²⁻	- 0.00764	0.01454	-0.53	0.612
AVS	- 0.06933	0.04129	-1.68	0.127
%OC	- 4.086	1.086	-3.76	0.004

764

765

766

767

768



769 **Table 3: Results of multiple regression analysis between surface layer CH₄ oxidation potential**
770 **([CH₄]_(ox)) vs. NH₄⁺ & NO₃⁻ concentrations .**

Predictor	Coef	SE Coef	T	P
Constant	1.6338	0.3253	5.02	0.015
NH ₄ ⁺	-0.3065	0.1362	-2.25	0.110
NO ₃ ⁻	0.2930	0.1285	2.28	0.107

771

772

773

774

775

776

777

778



779 **Table 4: Seasonal variation of dissolved CH₄ concentrations, physicochemical and biological**
 780 **parameters of estuarine water.**

Properties	Parameters	Position	Premonsoon	Monsoon	Postmonsoon
	[CH ₄] (nM)	Surface	54.20 ± 5.06	64.58 ± 10.56	90.91 ± 21.20
		Bottom	47.28 ± 12.85	53.27 ± 19.47	67.97 ± 33.12
Physical property	Temperature (°C)	Surface	29.99 ± 0.97	27.82 ± 0.26	19.88 ± 0.18
		Bottom	28.79 ± 0.07	26.92 ± 0.62	19.08 ± 0.78
	S _D (cm)		62.3 ± 13.1	29.7 ± 7.8	75.9 ± 7.7
Chemical properties	Salinity	Surface	27.09 ± 0.59	19.06 ± 4.33	22.33 ± 0.81
		Bottom	26.88 ± 0.15	18.87 ± 0.33	22.14 ± 0.65
	DO (mg L ⁻¹)	Surface	6.53 ± 0.29	6.04 ± 0.73	7.27 ± 1.14
		Bottom	5.83 ± 0.37	5.41 ± 0.03	5.98 ± 0.79
	pH	Surface	8.17 ± 0.16	8.10 ± 0.03	8.15 ± 0.06
Biological properties	Chl (μg L ⁻¹)	Surface	5.30 ± 0.19	3.11 ± 0.39	7.88 ± 1.90
	P (mg C m ⁻² hr ⁻¹)	Surface	56.9 ± 7.1	48.2 ± 8.0	88.0 ± 18.6
	R (mg C m ⁻² hr ⁻¹)	Surface	125.0 ± 100	102.8 ± 116.7	110.1 ± 65.6

781

782

783



784 **Table 5: Results of multiple regression analysis between [CH₄] and temperature (T) (°C), pH,**
 785 **chlorophyll (Chl) (µg L⁻¹), dissolved oxygen (DO) (mg L⁻¹), productivity and community**
 786 **respiration ratio (P / R).**

Predictor	Coef	SE Coef	T	P
Constant	-296.8	986.5	-0.30	0.792
T	-0.140	2.178	-0.06	0.955
pH	57.6	103.1	0.56	0.633
Chl	2.688	5.801	0.46	0.689
DO	-19.13	28.82	-0.66	0.575
P / R	8.50	61.86	0.14	0.903

787

788

789

790

791



792 **Table 6: Results of multiple regression analysis between dissolved methane consumption rate**
 793 **($[\text{CH}_4]_{\text{DOX}}$) vs. water temperature (T), salinity (S), dissolved oxygen (DO), DIN, net heterotrophy**
 794 **(P/R) and secchi disc depth (S_d).**

Predictor	Coef	SE Coef	T	P
Constant	-65.85	22.24	-2.96	0.031
T	0.7561	0.6142	1.23	0.273
S	2.1752	0.4949	4.40	0.007
DO	7.528	2.868	2.62	0.047
DIN	-0.4082	0.3686	-1.11	0.318
P/R	-2.012	2.938	-0.68	0.524
S_d	-0.30365	0.09738	-3.12	0.026

795

796

797

798

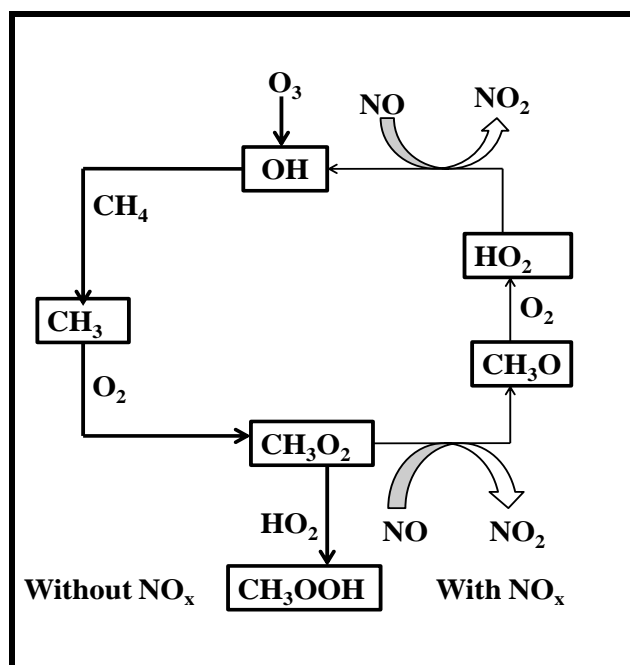


799 **Table 7: Seasonal variation of micrometeorological parameters, methane mixing ratio, biosphere**
 800 **– atmosphere CH₄ exchange and CH₄ photo-oxidation in mangrove forest atmosphere.**

Parameters	Height(m)	Premonsoon	Monsoon	Postmonsoon
Air temp. (°C)	10	30.34 ± 0.91	29.74 ± 2.50	17.34 ± 4.09
	20	29.73 ± 1.13	28.37 ± 0.88	16.17 ± 1.80
Wind velocity(ms ⁻¹)	10	0.70 ± 0.42	1.32 ± 1.11	0.41 ± 0.36
	20	0.95 ± 0.44	1.64 ± 1.37	0.80 ± 0.88
U* (m/sec)		0.20 ± 0.04	0.15 ± 0.15	0.17 ± 0.49
Z _o (m)		3.77 ± 3.01	1.63 ± 1.02	2.97 ± 2.98
C _{D(10m)}		0.386	0.157	0.167
H (W m ⁻²)		6.349	8.248	1.154
PBL (m)		936.59	702.45	796.10
CH ₄ (ppmv)	10	1.769 ± 0.04	2.180 ± 0.12	2.112 ± 0.05
	20	1.821 ± 0.09	2.027 ± 0.03	2.116 ± 0.06
F _{BA} (mg m ⁻² hr ⁻¹)		- 4.514	6.635	-2.110
[CH ₄] _{photo-ox rate} (molecules cm ⁻³ d ⁻¹)	10	1.40 x 10 ¹¹	1.67 x 10 ¹¹	6.05 x 10 ¹⁰

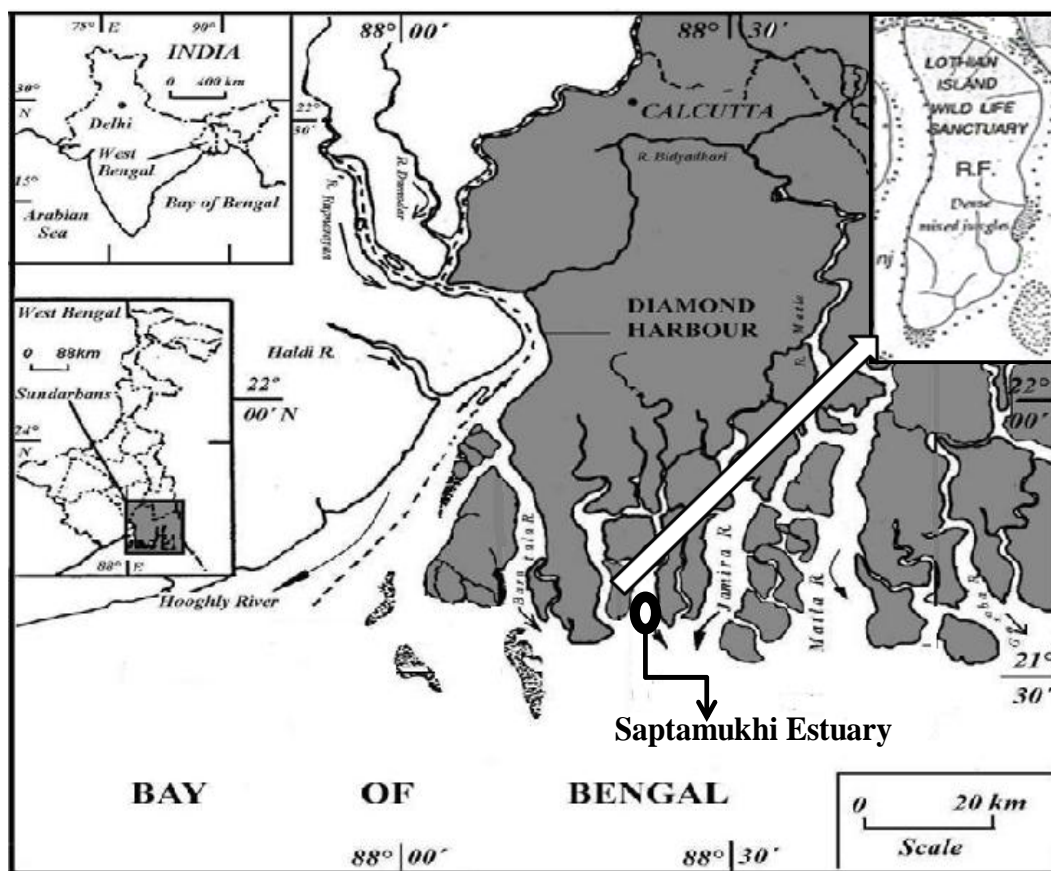


801



802

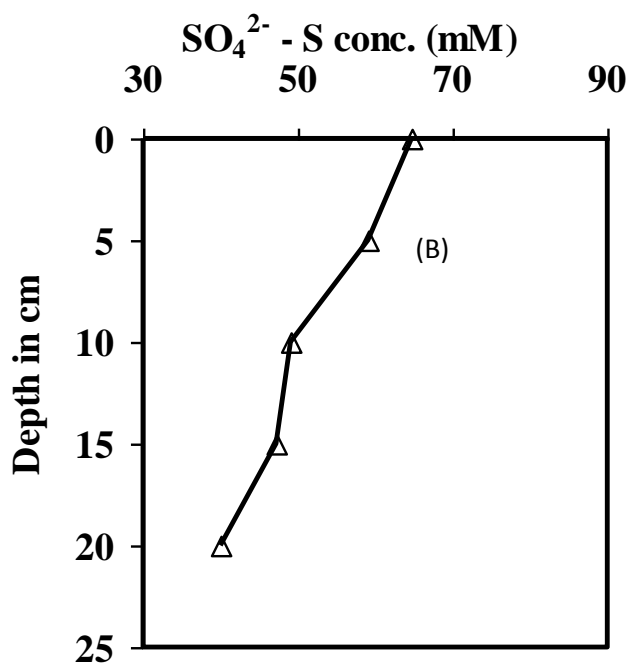
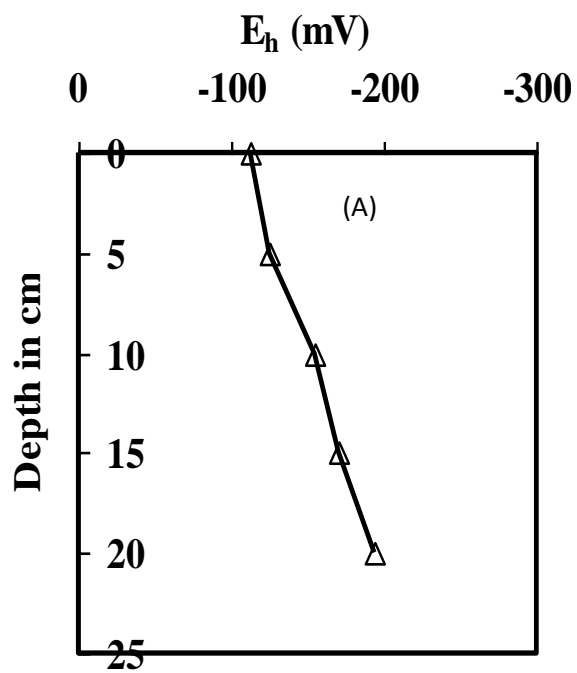
803 Fig.1: Schematic diagram of atmospheric CH₄ photooxidation with/without NO_x concentration.



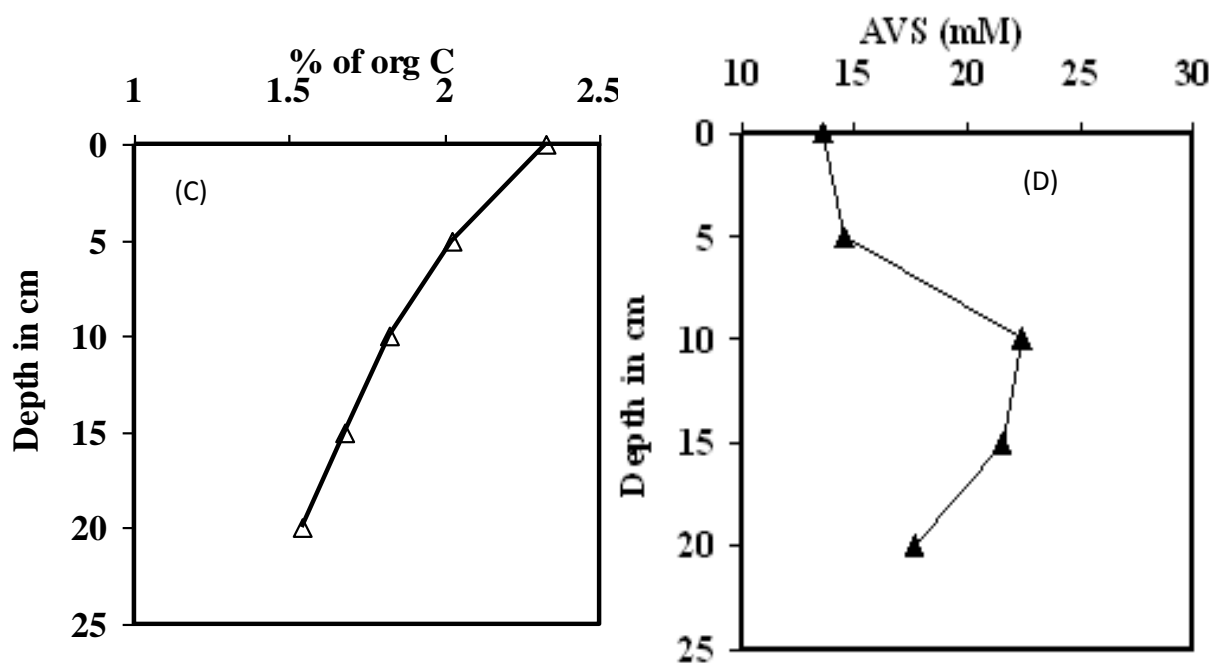
804

805

Fig.2: Map showing locations of the study point.

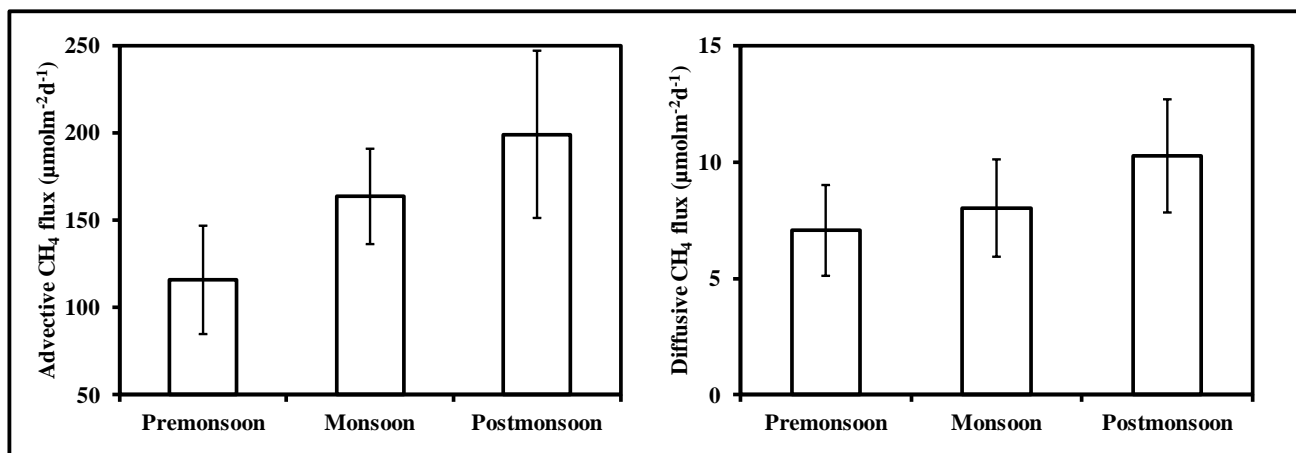


806

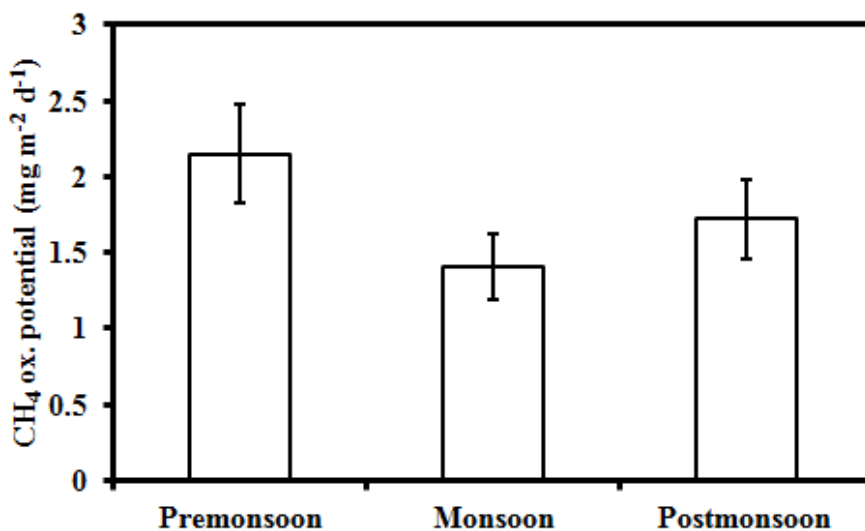


807

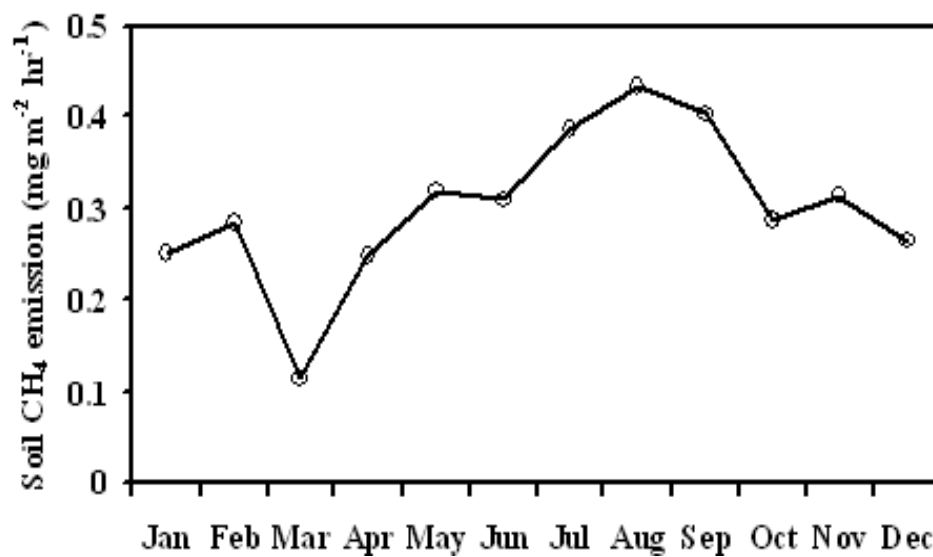
808 Fig.3: Vertical variation of physicochemical properties of mangrove sediment (A) E_h (B) pore water
809 sulphate – S concentration (C) % organic carbon (D) pore water AVS concentration



810
811 Fig.4: Seasonal variation of advective and diffusive CH₄ fluxes from intertidal and subtidal sediments,
812 respectively.

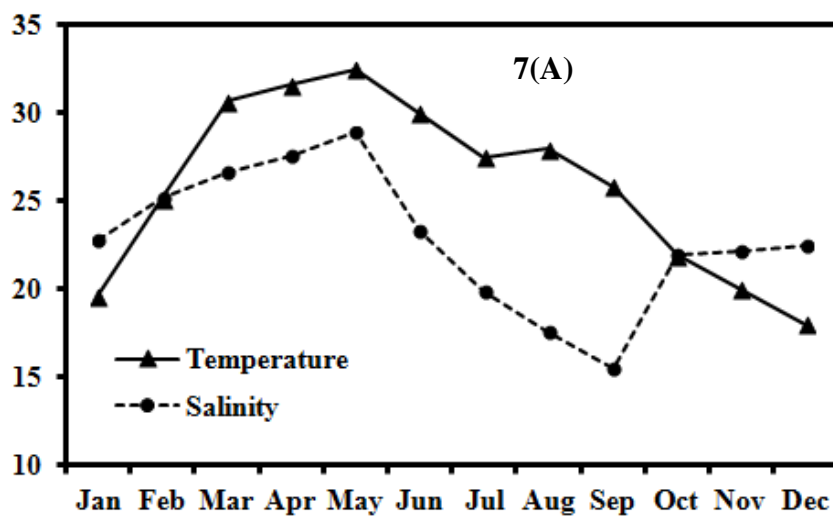


813
814 Fig.5: Seasonal variations of surface sediment CH₄ oxidation potential in mangrove sediment.

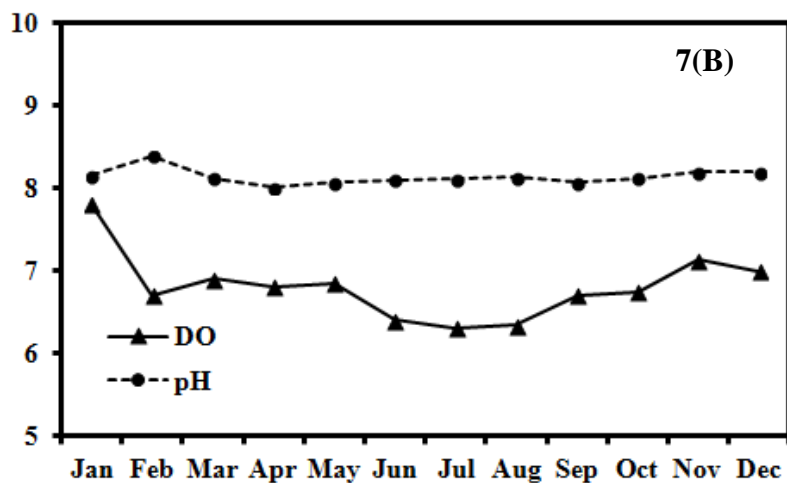


815

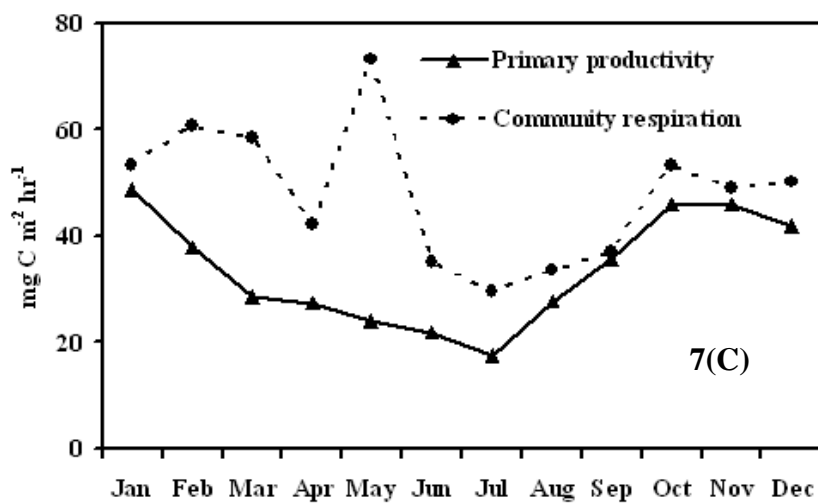
816 Fig.6: Monthly variation of soil methane emission from intertidal mangrove forest.

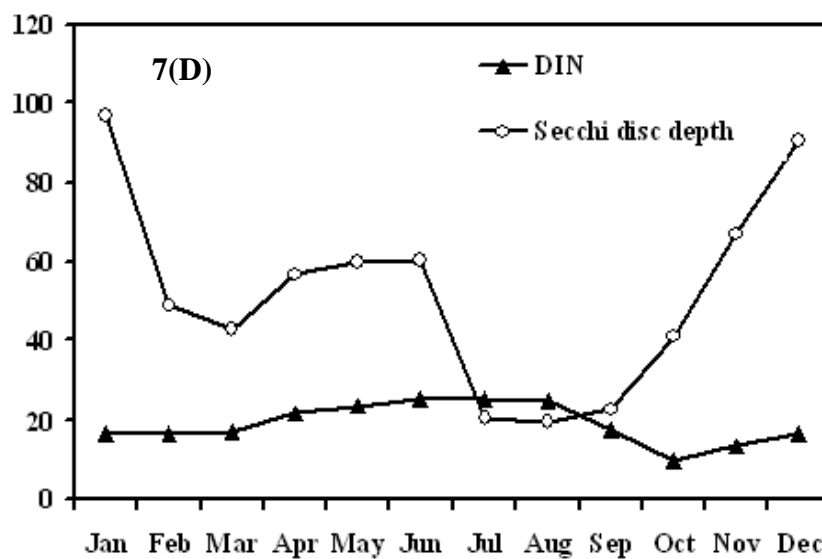


817

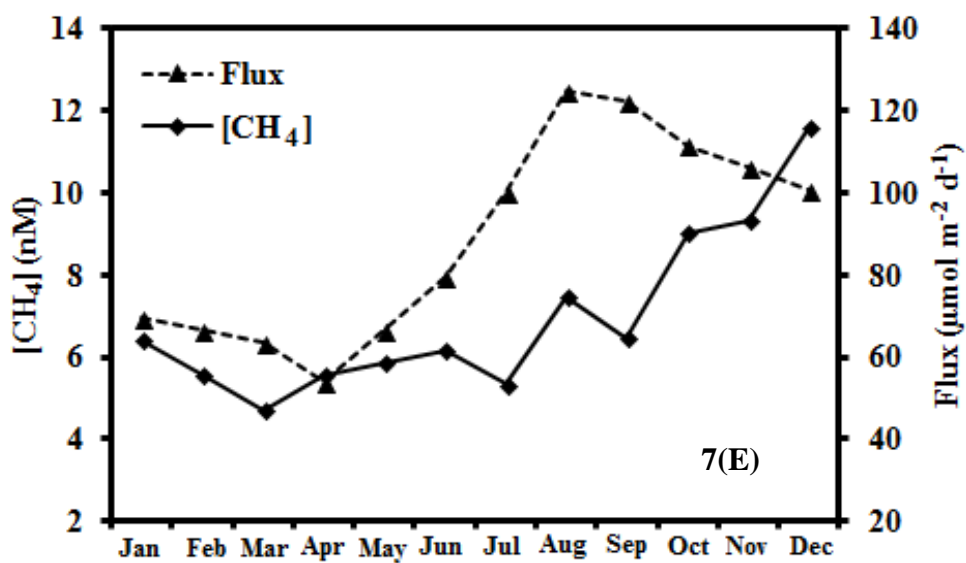


818



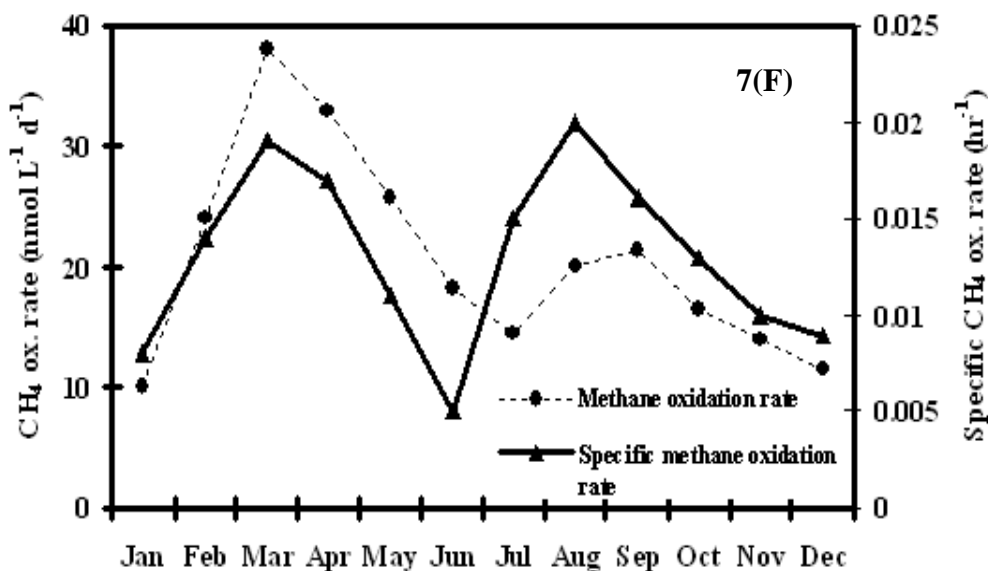


824



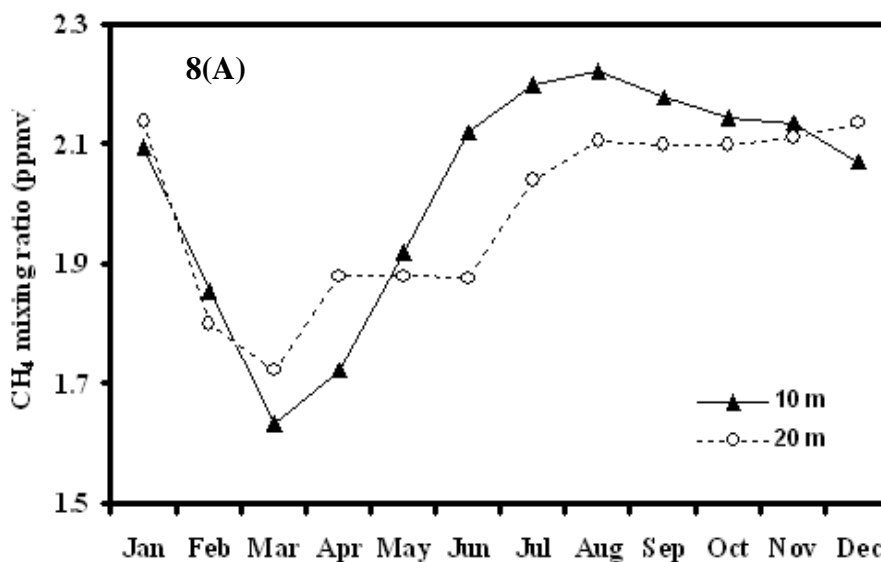
825

826

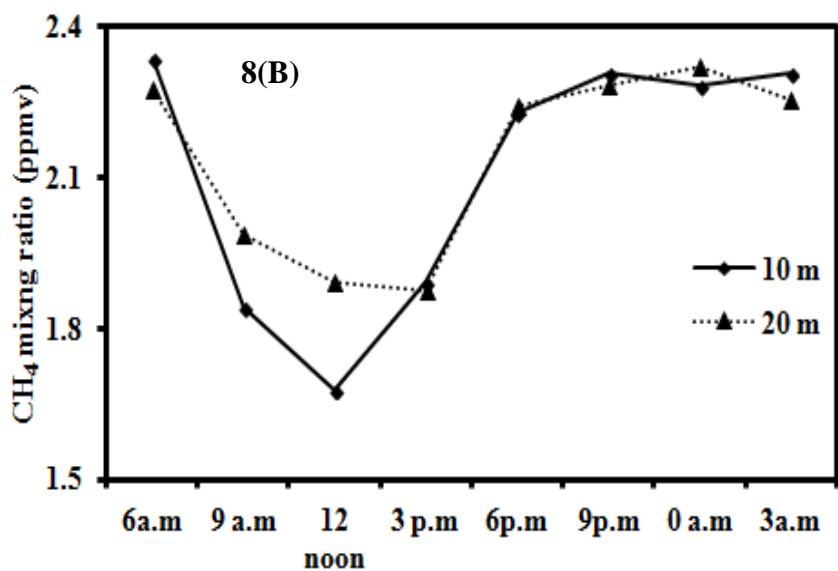


827

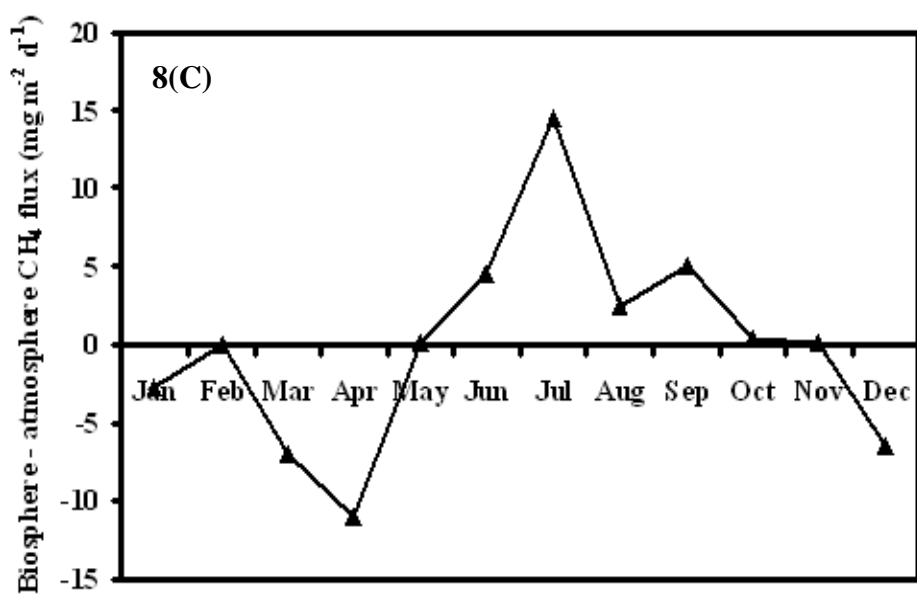
828 Fig.7: Monthly variation of physicochemical parameters along with dissolved methane concentrations,
 829 methane oxidation and air-water methane exchange flux.



830



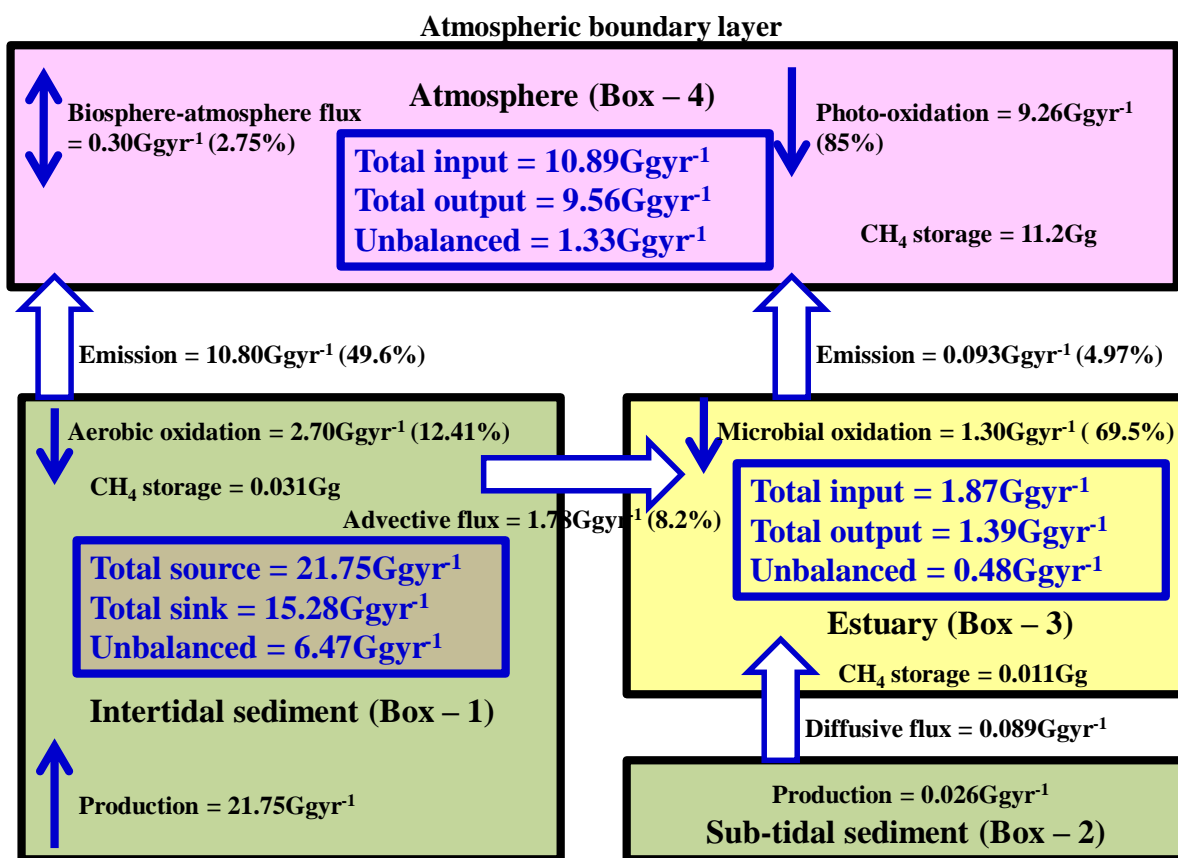
831



832



833 Fig.8: (A) Monthly variation of methane mixing ratio in forest atmosphere (B) Diurnal variation of
 834 methane mixing ratio in forest atmosphere (C) Monthly variation of biosphere-atmosphere methane
 835 exchange flux.



836

837 Fig.9: Quantitative methane budget at Sundarbans mangrove ecosystem.

838